

<https://doi.org/10.1038/s43247-025-02280-7>

Efficient agronomic practices narrow yield gaps and alleviate climate change impacts on winter wheat production in China

Check for updates

Kaiyuan Gong^{1,2,3}, Liangbing Rong^{3,4,5}, Yinghua Zhang⁶, Xiao Wang⁷, Fengying Duan³, Xia Li³, Zhihao He^{1,2}, Tengcong Jiang⁵, Shang Chen⁸, Hao Feng⁵, Qiang Yu⁵, Wenbin Zhou^{3,9}✉ & Jianqiang He^{1,2,9}✉

As the world's largest wheat producer, China's stable wheat production is crucial for global food security. However, climate change has increased yield variability, while excessive water and nitrogen (N) inputs threaten resource sustainability and environmental health. Here, we explored the possibility of yield gap reduction through efficient agronomic practices. A 3-year field experiment was conducted at 22 different sites in major wheat-producing regions in China, combined with modeling approaches to perform a comprehensive spatiotemporal analysis of wheat productivity. Results show that efficient agronomic practices could enhance wheat yields by about 7%-14% without expanding current cultivation areas in China. In the Huang-Huai-Hai region, adopting more efficient practices could reduce N fertilizer use by about 6% while maintaining current yields, thereby improving resource efficiency and minimizing environmental harms. This study highlighted the potential of optimized management strategies to enhance wheat production and reduce excessive resource inputs. The findings provided a scientific basis for developing sustainable agronomic practices in the major wheat-growing regions of China.

China is the world's largest wheat producer, accounting for 11% of the world's wheat area and 18% of world's total production¹. Winter wheat dominates (about 92%) of China's summer grain yield². Thus, the stability and sustainability in China's winter wheat production is crucial to ensure the food security for its 1.4 billion population and even for global agricultural development. However, the instability of wheat production has been exacerbated by climate change³. At the same time, China kept increasing inputs of water resource and nitrogen (N) fertilizer over the past several decades to increase production, which may lead to unsustainable resources and harm to the environments.

Due to the fast-paced development and urbanization in China, the shortage of population and land in agriculture has become a pressing issue. Given that the area for wheat production may not increase or even decrease in the future, the stability and growth of total wheat output in China will mainly depend on the increase of wheat per-unit yield. Yield gap analysis

provided a valuable tool to describe the effects of environmental changes and field measure improvements on wheat production and to estimate the difference between the current farm production and the potential production. Generally, narrowing the yield gap is an essential strategy to sustainably feed the growing population in China^{4,5}. Narrowing the yield gaps requires a comprehensive analysis of the yield disparities across different regions, followed by the development of targeted measures to reduce these gaps and enhance production in each specific region. In addition, climate change, particularly changes in precipitation and temperature, is expected to have negative impacts on crop production in China⁶⁻⁸. This complicates the issue about how to reduce yield gaps further. Since 1980, wheat yield in China has increased by over 60%, thanks to genetic improvement, environmental changes, and improved agricultural measures. Nonetheless, the growth trend in wheat production has slowed down in recent years as the impacts of climate change and water resource shortages partially offset the continued

¹Key Laboratory for Agricultural Soil and Water Engineering in Arid Area of Ministry of Education, Northwest A&F University, Yangling, Shaanxi, China. ²Institute of Water-Saving Agriculture in Arid Areas of China, Northwest A&F University, Yangling, Shaanxi, China. ³Institute of Crop Sciences, Chinese Academy of Agricultural Sciences, Beijing, China. ⁴College of Natural Resources and Environment, Northwest A&F University, Yangling, China. ⁵State Key Laboratory of Soil Erosion and Dryland Farming on the Loess Plateau, Institute of Soil and Water Conservation, Northwest A&F University, Yangling, China. ⁶College of Agronomy and Biotechnology, China Agricultural University, Haidian District, Beijing, China. ⁷National Technique Innovation Center for Regional Wheat Production/Key Laboratory of Crop Physiology, Ecology and Production, MOA/National Engineering and Technology Center for Information Agriculture, Nanjing Agricultural University, Nanjing, China. ⁸Jiangsu Key Laboratory of Agricultural Meteorology, Nanjing University of Information Science and Technology, Nanjing, China. ⁹These authors contributed equally: Wenbin Zhou, Jianqiang He. ✉e-mail: zhouwenbin@caas.cn; jianqiang_he@nwsuaf.edu.cn

per-unit yield rise caused by genetic improvement⁹. However, some previous studies often lacked clear definitions of yield gaps and were not supported by extensive regional data obtained from yield gap experiments. Most researches focused on quantifying yield gaps across different regions, without providing feasible solutions to narrow these gaps. To address these issues and achieve future wheat yield increase, the improvement of agronomic practices was proved to be the most feasible solution to narrow the yield gaps^{10–12}.

Some previous studies showed that there is still significant room for yield improvement through enhancing cultivation management practices. For instance, Rizzoa et al.¹³ analyzed the contributions of cultivars, cultivation practices, and climatic conditions to the increase of irrigated maize yield in the United States. They found that about 39% of the yield increase was attributed to the improvements of agronomic practices. Moreover, through increasing irrigation levels and improving nutrient management, it was possible to achieve yield increases by about 45–70% for the majority of crops⁴. One of the main factors that limit winter wheat yield and resource utilization efficiency is the lack of optimization of agricultural practices. Kheir et al.¹⁴ conducted field experiments to optimize wheat management practices in the main wheat-growing areas in Egypt and found that about 80% of the current irrigation volume was sufficient to maintain wheat yields while improving resource use efficiency. Additionally, yield projections under future climate change for the region suggested that optimized management practices could increase wheat yield by about 4.5% and also improve wheat quality¹⁵. Therefore, different agronomic practices were designed and applied at various yield levels in the station experiments. Generally, high planting density could increase solar radiation interception, enhance nitrogen accumulation after heading, and thus improve the yield of winter wheat^{16,17}. Low N application rate would reduce grain N content and yield and aggravate soil fertility depletion, while an excessive application N rate would reduce the production efficiency and increase environmental costs^{18–20}. One-time fertilization could increase the risk of N losses and seedling injuries^{21–23}. In addition, winter wheat cultivation in the Huang-Huai-Hai and Xinjiang regions in China usually required irrigations. Optimizing irrigation timing and frequency could increase yield and improve water use efficiency of winter wheat^{24,25}.

Currently, local governments in China have increased their investments in agriculture²⁶. China has implemented a series of policies to encourage wheat production and the use of fertilizers to meet the increasing demands of both yield and quality of wheat²⁷. However, excessive use would decrease the economic benefits and utilization efficiency of N fertilizer in wheat production, resulting in increased adverse environmental impacts from local to global scales and threatening human health²⁸. Therefore, it is an urgent priority for food security and environmental sustainability to reduce the harmful impacts of N fertilizer while maintain food production²⁹.

For instance, the Huang-Huai-Hai Plain is the most important wheat production base in China, supplying about 50% of the country's wheat production³⁰. This region is mainly affected by a monsoon climate, with precipitation concentrated in the summer and less in the spring. In order to enhance winter wheat yield in this region, it is a common practice to irrigate wheat fields with substantial volumes of water during the growing season, typically three to four times the crop water requirements^{31,32}, with most of the irrigation water coming from deep groundwater pumping^{33,34}. Over-exploitation of groundwater resources can lead to serious ecological and environmental problems, such as a continuous decrease in groundwater storage, rapid decline in groundwater levels, land subsidence, and seawater intrusion^{35–37}. Some previous studies demonstrated that excessive increases in water and N inputs in farmland management may not necessarily enhance crop yields in some regions but are likely to increase the potentials for ecological pollution^{38,39}. Some relevant studies also demonstrated that climate change will further exacerbate the negative impacts of agriculture on the ecological environment. There is an urgent need for a transition to climate-adaptive sustainable agricultural systems to mitigate the adverse effects of climate change on the global environment⁴⁰. Thus, it has very high

priority in China to implement water-saving, fertilizer-reducing, and high-yielding agronomic practices in wheat production⁴¹.

In this study, we hypothesized that it is possible to increase yields and narrow yield gaps while enhancing resource use efficiency through implementing reasonable agronomic practices, thus reducing the negative impacts on the ecological environment under future climate change scenarios⁴². To validate this hypothesis, we followed an “experiment + crop model + future climate change” methodology to estimate wheat yield gaps in China under various agronomic practices and climatic conditions. First, a three-year field experiment was conducted across major wheat-growing regions in China. The agronomic practice for the experiment was based on locally surveyed management practices and several years of management optimization trials. Although field experiments could help understand the interactions between crop management and the environment, they are usually confined to specific locations. Given the nonlinear interactions between and dynamics of local soil and climate conditions^{41,43}, it is challenging to identify the optimal crop management practices only through field trials. To determine the potential spatiotemporal variations of optimized management practices, this study employed a crop modeling approach to quantify the effects of water and N fertilizer on winter wheat yield and the resource utilization efficiency under different agronomic practices and climatic conditions. Process-based crop models can account for various agroecosystem processes and their interactions, including crops' complex and nonlinear physiological responses to climate and soil conditions⁴⁴. As a result, crop models were widely used for crop yield prediction, water and N flux simulation, environmental impact assessment, and the identification of optimal field management practices in different regions^{18,45,46}. Simultaneously, the crop models driven by global climate models can be used to quantify the extent to which climate change would affect crop yields. Such an approach could offer valuable insights for developing strategies to mitigate the adverse effects of climate change on agriculture and ensure sustainable crop production in the future^{47,48}.

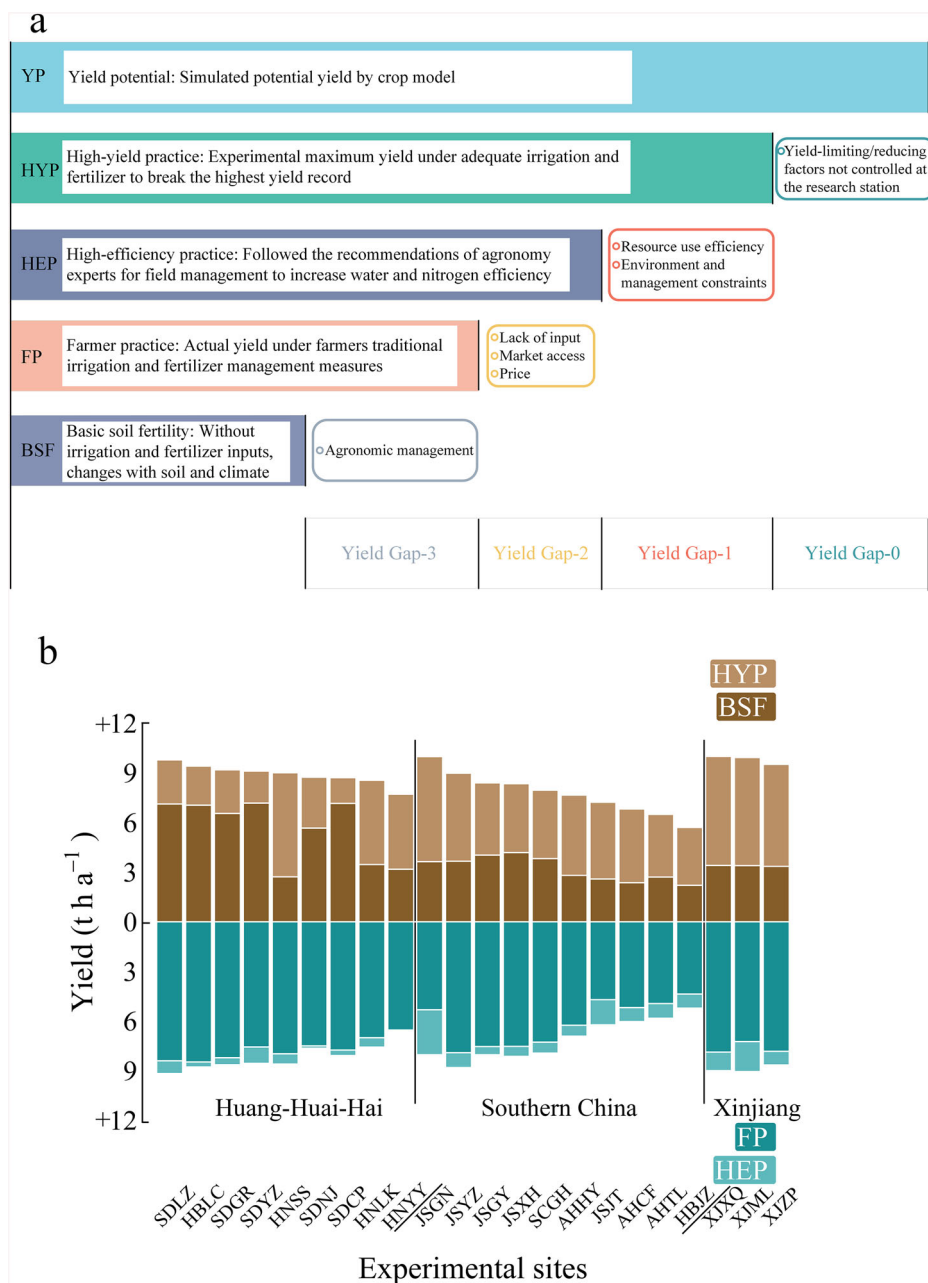
Specifically, we conducted a comprehensive experiment to investigate whether optimized management practices could effectively narrow yield gaps across three distinct periods of 1961–2020 (historical baseline period), the 2040 s (near future), and the 2080 s (distant future). This investigation was carried out through a combination of field experiments and model projections. The main objective was to evaluate the potential for yield increase, water conservation, and N reduction in wheat production under future climate change in China. Finally, several appropriate measures of water and N fertilizer management were proposed for winter wheat production, which are of great significance to ensuring sustainable national production of winter wheat in China.

Results

Current potential yield and yield gap of winter wheat

In this study, we defined five yield levels and four yield gaps for winter wheat production in China. A three-year field experiment was conducted at a total of 22 experimental sites nationwide for the four yield levels, among which yield potential was simulated by the crop model (Fig. 1a, Supplementary Table 1). Different agronomic practices were employed across these different yield levels. Obvious yield variations were observed among different experimental sites in the same wheat-producing region. The results demonstrated that the impacts of agronomic practices on yield differed across sites (Supplementary Fig. 1). In the Huang-Huai-Hai region, the baseline yield potential was higher than in Southern China and the Xinjiang regions. However, the yield gap between ‘High-yield practice’ and ‘Farmer practice’ levels in this region was smaller than the other regions (Fig. 1b). Site trials confirmed that agronomic practice improvements could enhance yield and reduce the yield gap of winter wheat, although the degrees of gap reduction varied across sites. In the three years, the trials demonstrated that effective agronomic practices were essential for agricultural production improvement. However, these results only reflected the differences in winter wheat yields among given years and specific sites. To comprehensively understand the long-term trends and national-scale wheat cultivation, a

Fig. 1 | Winter wheat yield levels and their main constraints in the 3-year field experiments. **a** Five different yield levels and four kinds of yield gaps were obtained based on field experiments and crop model simulations. **b** Field experiments of three years (2017–2019) were conducted at a total of 22 research stations (9 in the Huang-Huai-Hai Plain; 10 in Southern China; and 3 in Xinjiang), and different yield levels (HYP, BSF, FP, and HEP) were observed at these stations, respectively.



spatial upscaling was conducted simultaneously for the experimental results in this study through crop model and the protocols of Global Yield Gap Atlas (GYGA; www.yieldgap.org) (Fig. 2, Supplementary Figs. 2–6, Supplementary Table 2).

In this study, we analyzed yields and yield gaps of winter wheat across various agronomic practices over the past 60 years (1961–2020) nationwide. Additionally, we compared the differences of yields and yield gaps among the three main winter-wheat planting regions with different cultivation systems (Fig. 3). Generally, there were significant regional disparities among wheat yield gaps. Compared with the other regions, the Huang-Huai-Hai region, where wheat-maize rotation is the primary cropping system, had the highest wheat yield potential ($11.5\ t\ ha^{-1}$; Figs. 4, 5). This region also had the largest wheat planting area in China (about 60%; Fig. 3a). In contrast, the Southern China region, where rice-wheat rotation is the dominant cropping system, had the lowest yield potential for wheat ($8.6\ t\ ha^{-1}$; Fig. 5). However, the Xinjiang region, with scarce water resources, achieved the highest yield for the three production levels (i.e., High-yield practice, HYP; High-

efficiency practice, HEP; Farmer practice, FP) under them different agronomic practices tested at experimental sites, with an average HYP yield exceeding $8\ t\ ha^{-1}$. Under the conditions without irrigation and fertilization (i.e., Basic soil fertility), there were significant differences among the three regions, with the highest yield in the Huang-Huai-Hai region ($5.3\ t\ ha^{-1}$); in comparison, both Xinjiang and Southern China regions had winter wheat yields about $3.0\ t\ ha^{-1}$ (Fig. 5). This phenomenon generally reflected the overall suitability of crop variety, soil, and climate conditions for wheat production in the three different regions.

Currently, the yield levels were generally lower in the south and higher in the north across the three main winter-wheat planting regions in China. The areas with higher yields included the eastern Shandong Peninsula and the western Loess Plateau in the Huang-Huai-Hai region (Fig. 4). In the past 60 years, the coefficient of variation (CV) of yield potential of winter wheat was about 8.9%, indicating that the yield potential of winter wheat was more stable than the other yield levels under various climates, while the yield fluctuations were relatively higher at the ‘Farmer practice’ level

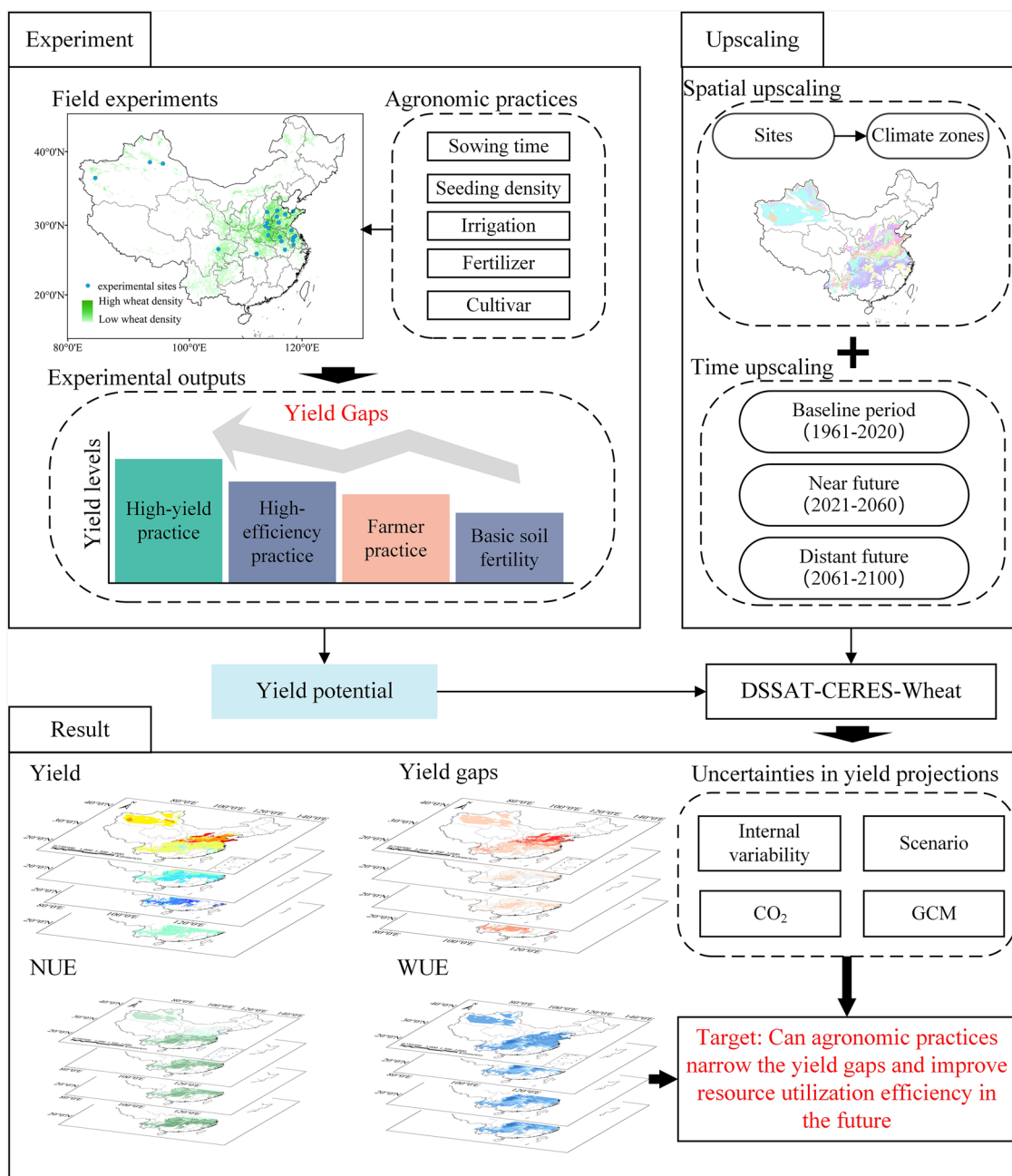


Fig. 2 | The simulation framework enables the optimization results of spatiotemporal scaling of agronomic practices.

(CV = 18.2%; Fig. 4). Among all of the yield levels, the central area of the Huang-Huai-Hai region had the highest yield variation (Fig. 4). Generally, climate change over the past 60 years benefited winter wheat production increase in China, but production-enhancing degrees varied in different producing regions and at different yield levels (Fig. 5). Some areas in the Southern China region experienced a production decrease at the ‘Yield potential’ (YP), ‘High-yield practice’ (HYP), and ‘High-efficiency practice’ (HEP) levels, while the other areas had a significant production increase. At the ‘Basic soil fertility’ (BSF) and ‘Farmer practice’ (FP) levels, only a few areas in the Huang-Huai-Hai and Xinjiang regions had increased winter wheat yields. Generally, as the yield level was higher, the magnitude of yield changes was greater and the affected area was larger under different agronomic practices (Figs. 4 and 5).

Currently, China’s national winter wheat yield at the “FP” level reached about 69.5% of the yield ceiling, and further increase in management inputs would improve the yield up to about 78.9% of the yield ceiling (Fig. 6d). The

remaining yield gap was mainly caused by uncontrollable yield-reduction factors such as diseases, insects, and weeds in the cropping system at the experimental sites. At the national scale, improving resource use efficiency through agronomic practices could narrow the yield gap by about 4.7% (YG-1), and increasing resource input could also narrow the yield gap by the same amount (YG-2). The disparity between YG-3 and YG-0 was greater than that between YG-3 and YG-1 (Fig. 6, Supplementary Table 5). This indicates that the most direct way for China’s wheat to narrow the yield gap is to implement agronomic practices from scratch and invest without considering costs. At the regional scale, the northern area of the Huang-Huai-Hai region had a higher yield gap for YG-0, while Xinjiang had a higher yield gap for YG-3 over the past 60 years (Fig. 7), indicating that future input of irrigation and fertilization could improve wheat yield in these areas. However, the achievable yield at the ‘HYP’ level still had a considerable gap from the ideal yield ceiling. In the Loess Plateau of the Huang-Huai-Hai region, the yield gap of YG-1 was higher, but YG-2 was lower than in the other areas,

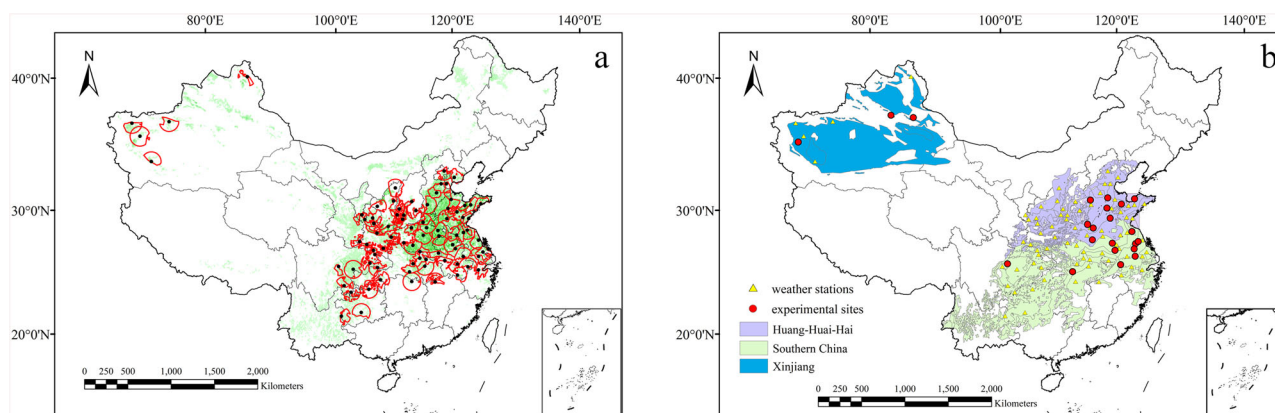


Fig. 3 | Selected reference weather stations (RWS) and the experimental sites in the three main wheat producing areas (Huang-Huai-Hai, Southern China, and Xinjiang) of China. a RWS and their buffer zones which were selected according

to the descending order of covered wheat harvest areas; **b** Experimental sites distributed climate zones (CZ) in each region.

indicating that it could not help achieve higher yields at the ‘FP’ level based on water and N use efficiency improvement through agronomic practices in this area. On the contrary, the yield gap of YG-2 in the Southern China region was higher than in the other regions (Figs. 6 and 7), indicating that improving resource use efficiency through agronomic practices could dramatically increase the yield and narrow the winter wheat yield gap.

Climate-induced changes in wheat yield and yield gaps across the five levels of agronomic practices

Projections of wheat yield changes were conducted for five yield levels and four different yield gaps while considering the impacts of CO₂ since CO₂ changed simultaneously and gradually under different future climatic scenarios (Fig. 5 and Supplementary Fig. 7). Average yield levels and yield potential of each agronomic practice level were summarized for the two different scenarios (SSP245 and SSP585) in two future periods (2021–2060 and 2061–2100) (Fig. 2). The predicted wheat yields under improved agronomic practices (i.e., HYP and HEP) and under ‘YP’ conditions showed obvious differences among different scenarios and years, while the predicted winter wheat yields were similar under the ‘BSF’ and ‘FP’ practices (Supplementary Fig. 8, Supplementary Table 5). Spatially, wheat yield predictions under the ‘BSF’ condition showed few differences, except for the Shandong Peninsula, with a relatively higher yield. However, the distributions of high-yield areas were consistent spatially in the other predictions of winter wheat yields, mainly concentrating in the northern and eastern parts of the Huang-Huai-Hai and Xinjiang regions. Spatial differences in predicted average yields of winter wheat were greater in different time periods than under different future scenarios. Under the scenario of SSP585 in 2061–2100, yield potential in high-yield regions generally exceeded 14 t ha⁻¹, while wheat yields also reached this level in some areas under the ‘HYP’ level. Compared to the baseline period of 1961–2020, there were obvious differences between SSP245 and SSP585 scenarios in the changes of winter wheat yields (Fig. 4, Supplementary Fig. 8a). Especially in 2040 s (2021–2060), most parts of the main producing regions had a remarkable increase in winter wheat yields. The area and magnitude of yield enhancement were both greater than in 2080 s. Additionally, this study highlighted the impact of CO₂ on winter wheat yield and reflected that future changes in CO₂ concentration would also be a key factor influencing winter wheat production. In contrast, Obvious variations were found in the spatial distributions and trends of projected winter wheat yields under the CO₂ concentration unchanged (CO₂ [416 ppm], Supplementary Fig. 9a). During the period of 2061–2100, some areas experienced a decline in production (Supplementary Figs. 9b and 10). This reflects the contribution of CO₂ to future wheat yields. In the future, YG-0 and YG-3 yield gaps showed higher values and increasing trends in the whole China. Among them, YG-0 showed a clear increase under the SSP585 scenario in 2080 s compared with the baseline

period of 1961–2020. The spatial distributions of YG-1 and YG-2 remained relatively unchanged in future predictions of winter wheat yields. In some parts of Southern China, the yield gap of YG-1 was less than 0, indicating that the yield gap could be narrowed through more resource-efficient management measures (Fig. 7 and Supplementary Fig. 11). In some parts of the Huang-Huai-Hai region, the yield gap of YG-2 was less than 0, suggesting that there was no yield gap between the ‘FP’ and ‘HEP’ levels. The upscaling analysis also reflected this phenomenon (Figs. 6 and 7). In addition, the results of the geographic upscaling analysis indicated that the yield gap of YG-3 in the Xinjiang region had the highest value among all yield gaps, reaching about 5 t ha⁻¹ in future yield predictions, indicating a considerable potential for wheat yield increase in this region in the future. However, among all future wheat yield predictions, the yield gap increased dramatically under the SSP585 scenario in 2061–2100, highlighting the urgent need to narrow yield gap in the future under high greenhouse gas emission (Fig. 6). Additionally, the yield gaps in 2040 s were similar across different scenarios (Supplementary Fig. 12).

The average yield gaps of YG-2 in the Huang-Huai-Hai and Xinjiang regions were 0.5% and 1.0%, respectively (Fig. 6d), which indicated a limited potential to narrow the yield gap through improving agronomic practices as at the ‘FP’ level. However, the yield gap of YG-2 in the Southern China region was about 10.2% (Fig. 6d), suggesting a great potential to narrow the yield gap through efficient agronomic practices in the next 40 years. In contrast, the predicted yield gaps showed considerable differences between the two scenarios of SSP245 and SSP585 in the 2080 s. In the Southern China region, the yield gap of YG-0 under the changing CO₂ concentration and SSP585 scenario was higher (reaching 27.1%) than those under other simulation scenarios (Supplementary Fig. 12e), indicating an increased room to narrow the yield gap. In addition, under this simulation scenario, the yield gap of YG-1 in Xinjiang increased to 11.7% (Supplementary Fig. 12f), indicating more room to reduce the yield gap than the other simulation scenarios.

Spatial pattern of resource utilization efficiency across the four levels of agronomic practices

This study calculated the water use efficiency (WUE) and nitrogen use efficiency (NUE) under different agronomic practice levels in winter wheat production at three yield levels (Figs. 8, 9, Supplementary Figs. 13–15, 17). The results showed that different calculation methods for nitrogen use efficiency, including the fertilizer partial factor productivity (PFP) and the nitrogen agronomic efficiency (NAE), reflected the same significant differences across various wheat-growing regions (Fig. 9a). This demonstrated that efficient agronomic practices could significantly improve nitrogen use efficiency in winter wheat growth. The results also showed the Huang-Huai-Hai region had the lowest NUE, while the Southern China region had the

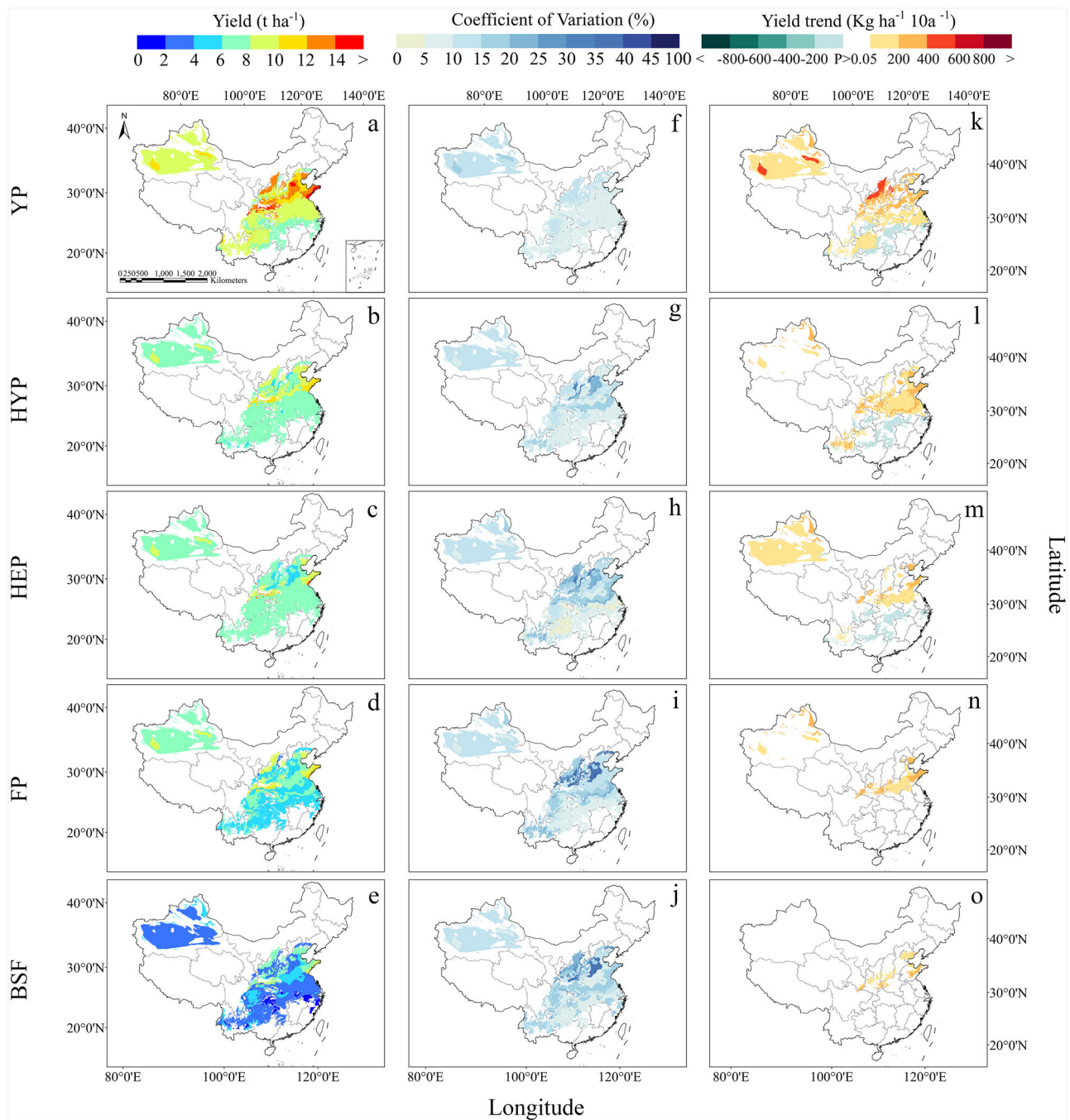


Fig. 4 | Five yield levels of winter wheat in China during the baseline period of 1961–2020. a–e Show the absolute values for YP Yield potential, HYP High-yield practice, HEP High-efficiency practice, FP Farmer practice, BSF Basic soil fertility;

f–j present the values of (coefficient of variation (CV) corresponding to the five yield levels; k–o depict yield trends (10-year average yield change rate), with blank areas indicating the non-significant in winter wheat yields ($P < 0.05$).

highest NUE among the three major producing regions in 1961–2020. In the Huang-Huai-Hai and Southern China regions, fertilizer partial factor productivity (PFP) was the highest at the ‘HEP’ level, then at the ‘HYP’ and ‘FP’ levels. In the Huang-Huai-Hai region, the PFP (fertilizer partial factor productivity) at the “HYP” level accounted for about 60% of the PFP at the “HEP” level, while the PFP at the “FP” level accounted for about 78% of the PFP at the “HEP” level. In contrast, in the Southern China region, the PFP at the “HYP” level accounted for about 79% of that at the “HEP” level, while the PFP at the “FP” level was close to the PFP at the “HEP” level.

The NAE (nitrogen agronomic efficiency) values at the “HYP” and “FP” levels were similar in the Huang-Huai-Hai and Southern China regions when the influence of soil was neglected and only the agronomic

practices were considered (Fig. 9, Supplementary Table 6), indicating that nitrogen use efficiency under the current level of farmer management was identical to that under the high-input management level. In Xinjiang, as irrigation and N fertilizer application increased, both PFP (partial factor productivity) and NAE (nitrogen agronomic efficiency) decreased (Fig. 9d). This was because Xinjiang is an extremely arid region in China despite good light and temperature conditions. Thus, continuous increase in N fertilizer input could narrow the winter wheat yield gap but would inevitably decrease the NUE in this region.

During the baseline period of 1961–2020, NAE showed an upward trend. Under the SSP585 and SSP245 scenarios, NAE (nitrogen agronomic efficiency) increased further in three main winter wheat producing regions

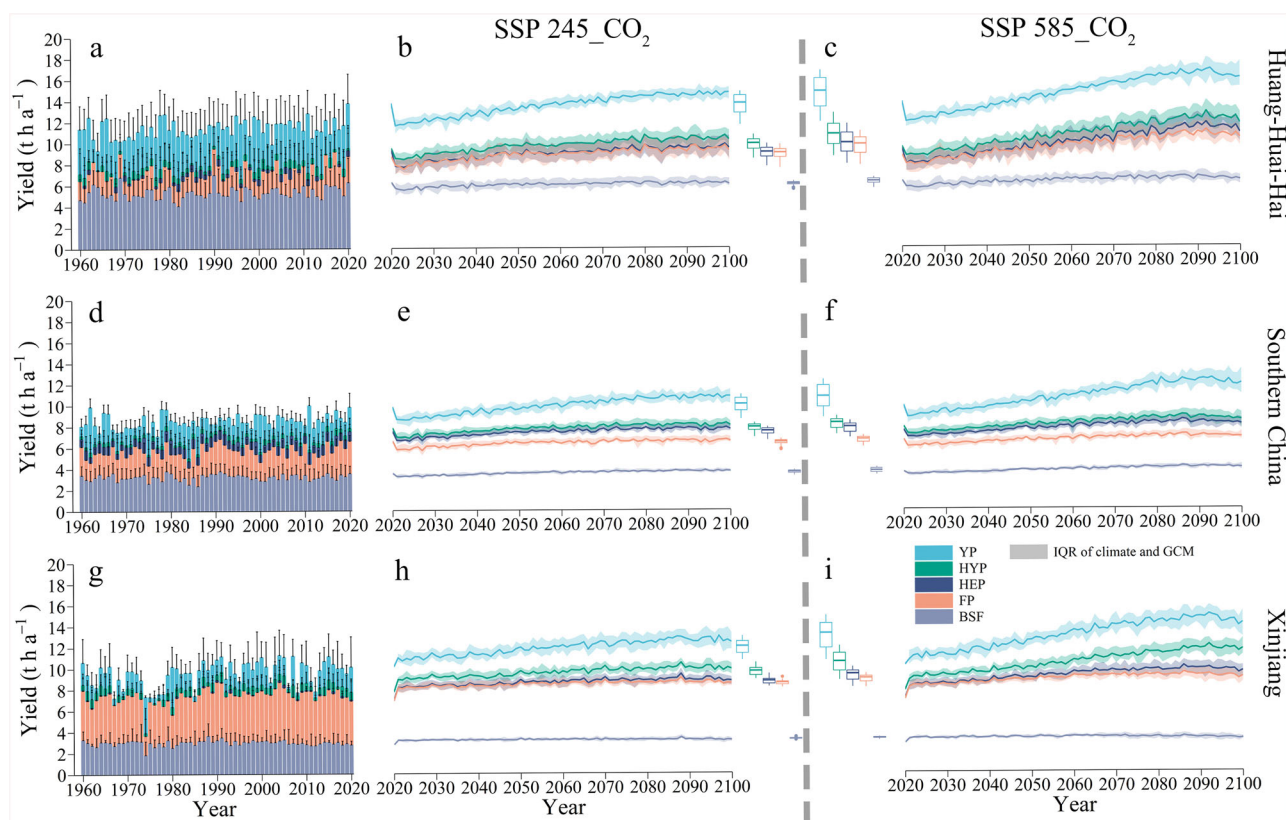


Fig. 5 | Winter wheat yield levels in three main winter-wheat regions (i.e., Huang-Huai-Hai, Southern China, and Xinjiang) of China during the baseline period (1961–2020) and projected average yields under SSP245 and SSP585 scenarios. a, d, g Show the absolute values of five different yield levels (YP Yield potential, HYP High-yield practice, HEP High-efficiency practice, FP Farmer practice, BSF Basic soil fertility) during the baseline period (1961–2020); **b, e, h** and **c, f, i** present the

average yields projected based on the multi-GCM ensemble in the period of 2021–2100 under SSP245 and SSP585, respectively. Shaded ranges illustrate the interquartile range (IQR) of all global climate models (GCMs). The solid lines show the mean response curves (**b, c, e, f, h, i**). Box boundaries indicate the 25th and 75th percentiles; the line within each box marks the median; whiskers below and above the box indicate the 10th and 90th percentiles, respectively.

(Fig. 9, Supplementary Table 6). NAE values at the “HEP” level in the Huang-Huai-Hai region increased at a remarkably higher rate under SSP585 than under SSP245. However, only under the SSP585 scenario did NAE show a decreasing trend after 2090 (Fig. 9b). Regarding spatial distributions, except for the Xinjiang region, NAE gradually increased from north to south over the past 60 years. The NAE at the “HEP” level in the middle and lower reaches of the Yangtze River Plain was even higher than that at the “HYP” and “FP” levels (Fig. 8). Compared with the baseline period of 1961–2020, the projected NAE was similar under the SSP585 and SSP245 scenarios, while the Southern China region had relatively higher NUE values. This suggested that optimized agronomic practices in Southern China could lead to more significant improvements in winter wheat yield and nitrogen use efficiency than other regions in the future.

In contrast to NUE, various agronomic practices exhibited comparable water use efficiency (WUE), although the Huang-Huai-Hai and Xinjiang regions are water-scarce (Fig. 8 and Supplementary Fig. 17, Supplementary Table 6). Thus, similar irrigation levels were required to ensure winter wheat growth in these two regions. Only WUE_i showed clear differences in the Huang-Huai-Hai region at different agronomic practice levels (Supplementary Fig. 13a). The “FP” level had the highest WUE_i, whereas the “HYP” level had the lowest WUE_i, indicating that the region’s overall WUE_i was substantially elevated. Consequently, rising irrigation levels were unlikely further enhance WUE_i. In Southern China, where water resources (such as precipitation) were abundant, irrigation was not applied in agronomic practices, leading to higher WUE under high-yield conditions. Due to the lower yield at the “FP” level in the Southern China region, the WUE was remarkably lower than that at the “HEP” and “HYP” levels. Xinjiang was a special winter wheat-producing region due to its historical labor and water

shortages⁴⁹, which was actually not a traditional winter wheat planting region in China^{50,51}. However, due to the good solar and thermal resources and advancement in agricultural irrigation technology, especially the heavily promoted technique of drip irrigation, winter wheat cultivation was permitted and rapidly expanded in Xinjiang. This study found that despite the high cost of drip irrigation technology, most water in winter wheat production was provided through the drip irrigation systems, resulting in a lower WUE_i than in the Huang-Huai-Hai region. Moreover, the WP (water productivity) and WUE_u in Xinjiang were also slightly lower than those in the Huang-Huai-Hai and Southern China regions. This was due to the higher solar radiation and temperature conditions in Xinjiang, which could increase the evapotranspiration (ET) and subsequently reduce the WUE_u^{52,53}. Based on the projections under the SSP585 and SSP245 scenarios, the increase in winter wheat yield would also boost in future WUE_u. However, the increase of WUE_u under SSP585 scenario was higher than that under the SSP245 scenario in the Huang-Huai-Hai region and at the “HYP” level in the Xinjiang region (Supplementary Fig. 14). Regardless of the baseline or future periods, the spatial distributions of WUE_u remained the similar, with higher values in the northern part of the North China Plain in the Huang-Huai-Hai region and the Sichuan Basin in Southern China.

Contributions of different sources to the uncertainties in climate change impact projections

There were usually considerable uncertainties in the productions of future winter wheat yields. For the three main producing regions and five yield levels of winter wheat, we partitioned the total uncertainties in wheat yield predictions into four main different uncertainty sources of CO₂, global climate models (GCMs), climate scenarios, and internal variations (Fig. 10).

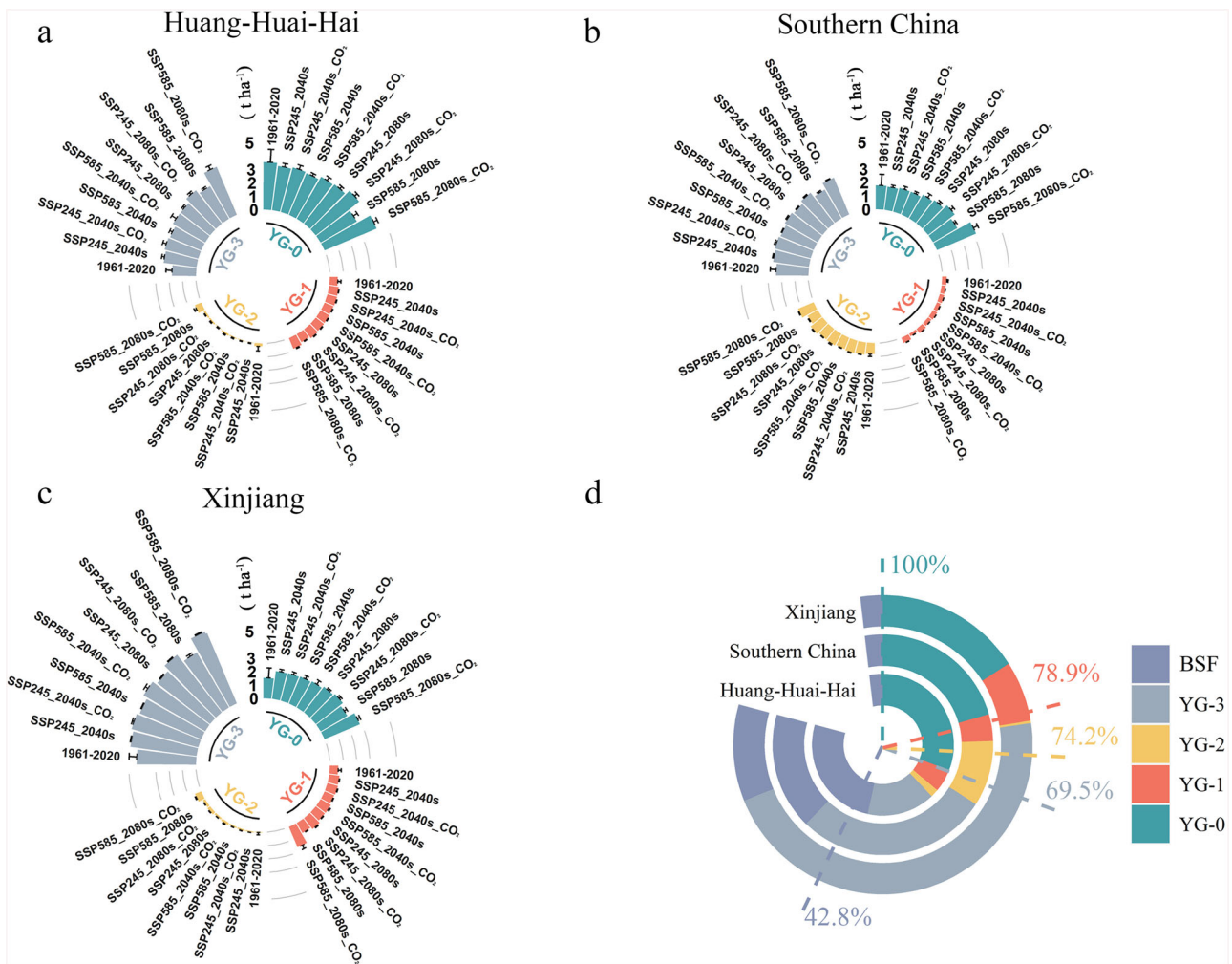


Fig. 6 | Current and projected yield gaps (YG-0, YG-1, YG-2, and YG-3) of winter wheat in the three main producing regions (i.e., Huang-Huai-Hai, Southern China, and Xinjiang) of China. Yield gaps are reported as absolute values (a–c) or as percentages of the potential yield in the baseline period of 1961–2020 (d).

Winter wheat yield gaps were projected based on an ensemble of 27 different global climate models (GCMs) in two future periods of 2040s (2021–2060) and 2080s (2061–2100) under the SSP245 and SSP585 scenarios at stable and changing CO₂ levels.

In some recent studies about wheat yield predictions, GCMs were proven to be the greatest uncertainty contributor, accounting for over 50% of the total projection uncertainties. This indicated that different climate models could dramatically influence the predictions of winter wheat yields. The uncertainty contribution from GCMs gradually decreased over time in three main winter wheat-producing regions, but the GCMs still dominated the uncertainties in winter wheat yield predictions at the end of the century. The projection uncertainties caused by the greenhouse gas emission scenarios and CO₂ concentrations could be neglected in the early predictions of winter wheat yields, but the uncertainty contribution by CO₂ concentrations gradually increased and could account for more than 60% of the total projection uncertainty by the end of this century. This could be explained by the fact that the influence of future anthropogenic greenhouse gases (CO₂) would increase dramatically after 2050 in China⁵⁴. For the predictions of winter wheat yields in the Huang-Huai-Hai and Xinjiang regions, the uncertainty caused by the greenhouse gas emission scenarios gradually increased, although this phenomenon varied at different agronomic practice levels. Specifically, the uncertainty contribution from the scenario gradually increased to about 10% in 2080–2100 at the “HYP”, “HEP”, and “FP” levels in the Huang-Huai-Hai region and the “YP” level in the Xinjiang region. Additionally, the uncertainty contribution from the scenario could be ignored in winter wheat yield predictions under other conditions. The uncertainty contribution from internal variations was around 20% in the

early period of the 21st century, but it became less than 5% in most areas by the end of the 21st century. This was because natural climate system fluctuations had a greater impact on near-term climate change, but such influence would decrease with time^{55,56}. The results suggested that GCMs were the dominant uncertainty contributor in near-term winter wheat yields projections, but the uncertainty contribution by CO₂ concentrations would dominate long-term projections of winter wheat yields.

Discussion

Agronomic-practices-dependent responses of winter wheat yields to climate change

Changes in China’s winter wheat production would greatly impact global wheat trade, which highlighted the urgent need for accurate estimates of yield variations in current wheat-producing regions in China. Thus, high-spatial-resolution analyses of winter wheat yield gaps in different climatic zones and cultivation systems were essential to adequately inform policy-makers and agricultural planners about future food security and land use in China. For this reason, this study (i) differentiated five yield levels for winter wheat production in China; (ii) categorized the primary wheat cultivation systems in the three main winter wheat producing regions (i.e., Huang-Huai-Hai, Southern China, and Xinjiang); (iii) conducted future winter-wheat yield projections with the DSSAT-CERES-Wheat, a wheat growth simulation model that were rigorously validated for its ability to estimate

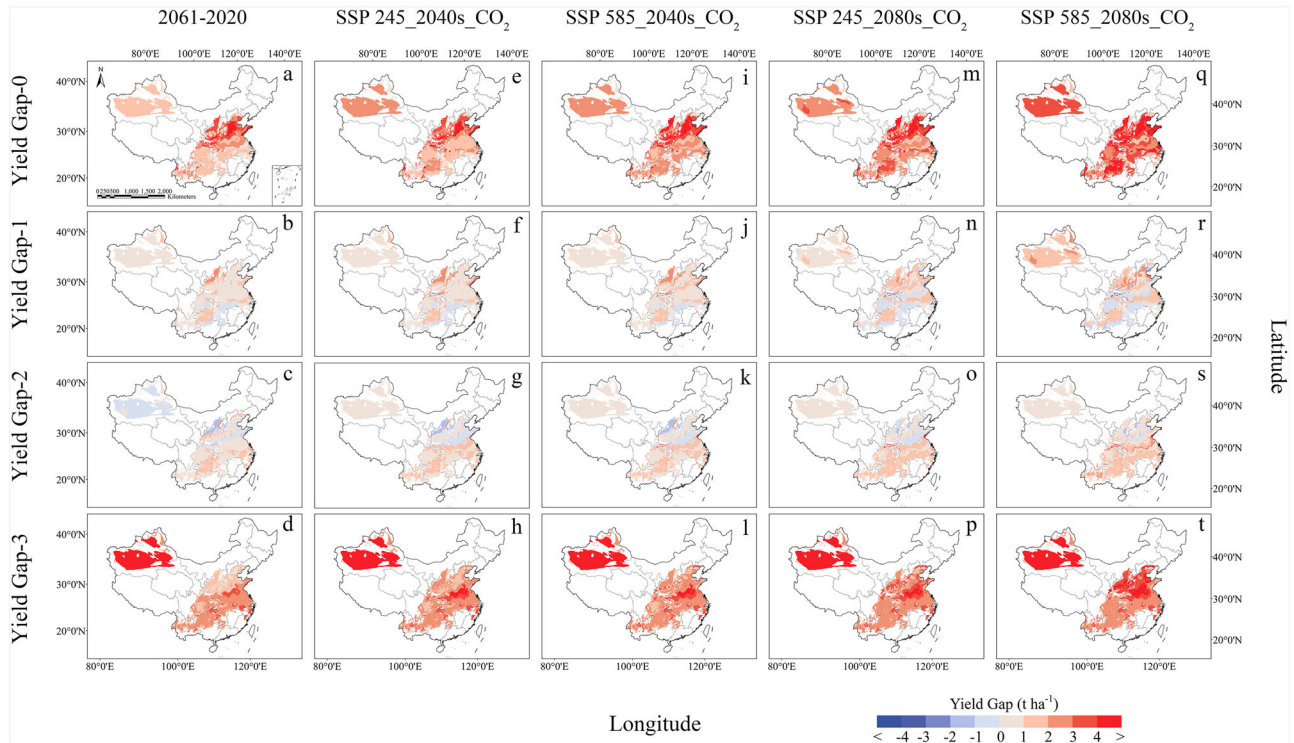


Fig. 7 | Average yield gaps of winter wheat in China. Column panels show the average yield gaps during the baseline period of 1961–2020 (a–d), and the average yield gaps under two scenarios of SSP245 and SSP585 in future periods of 2040 s (e–l) and 2080 s (m–t) in the three winter-wheat producing regions (Huang-Huai-

Hai, Southern China, and Xinjiang) of China. Negative values of YG-1 and YG-2 indicate that the yield at HEP (‘High-efficiency practice’) level was higher than at the HYP (‘High-yield practice’) level and lower than at the FP (‘Farmer practice’) level.

Fig. 8 | Nitrogen agronomic efficiency (NAE) and water use efficiency (WUE_u) at three different yield levels in China during the baseline period of 1961–2020. a–c Show the absolute values of NAE for the HYP High-yield practice, HEP High-efficiency practice, FP Farmer practice, yield levels; d–f present the absolute values of WUE_u for the same three yield levels.

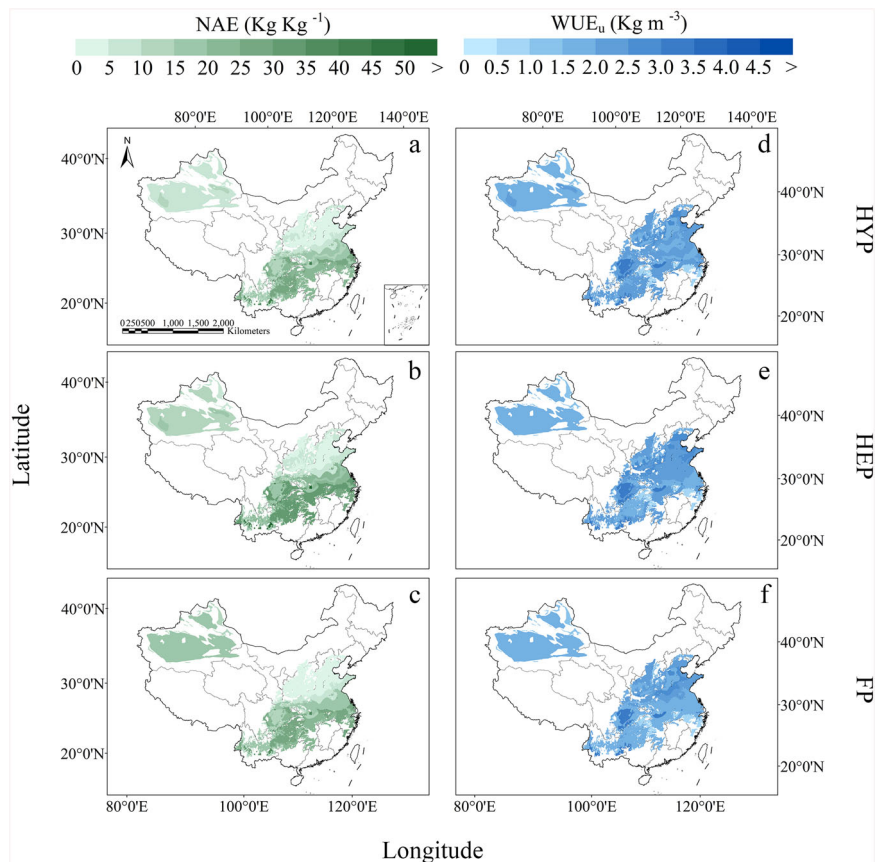
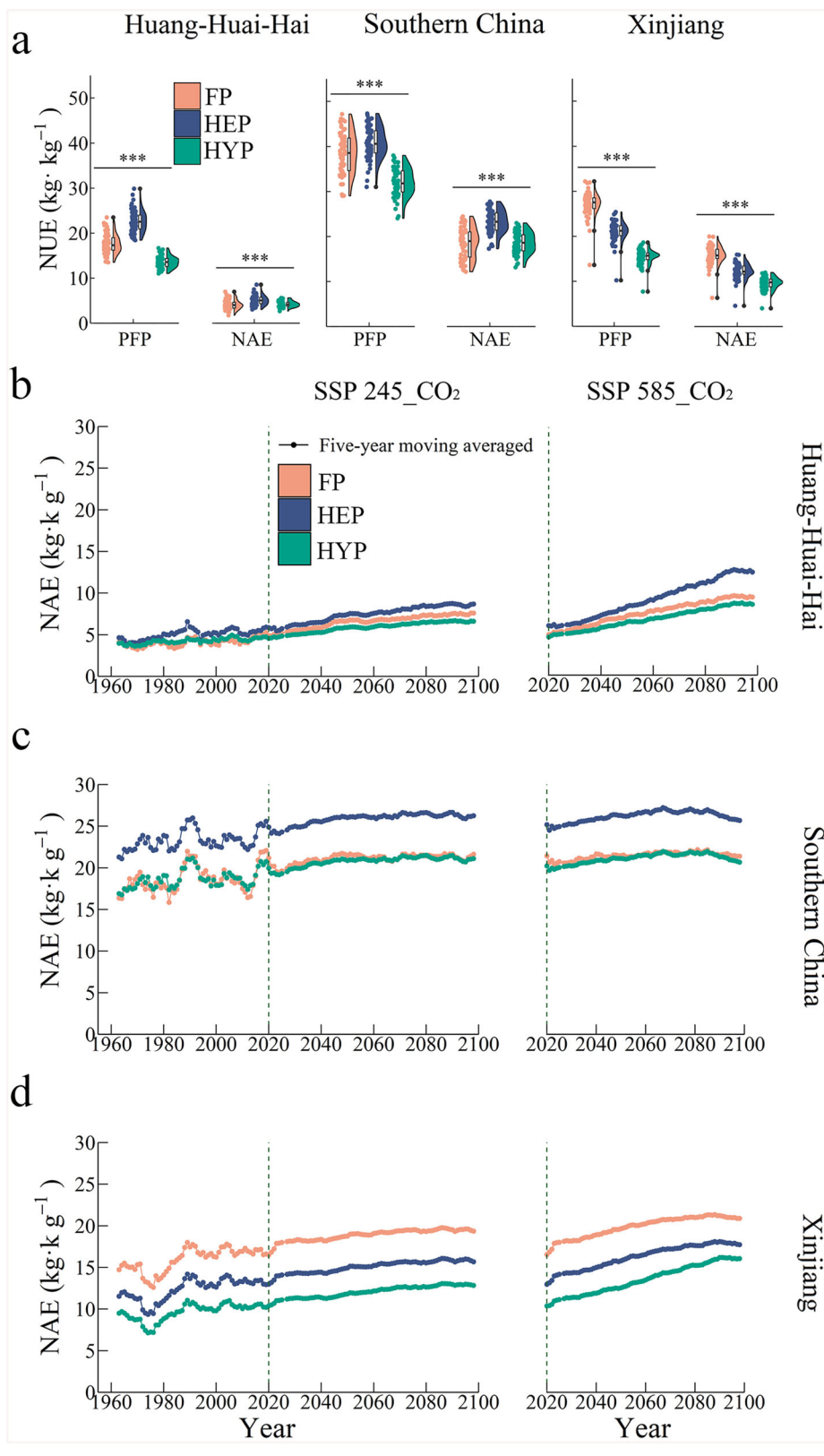


Fig. 9 | Nitrogen use efficiency (NUE) of winter wheat for different levels of agronomic practices in three main producing regions (i.e., Huang-Huai-Hai, Southern China, and Xinjiang) of China. a Panels show the NUE during the baseline period of 1961–2020 ($n = 60$). The plots display mean horizontally jittered values of PFP (fertilizer partial factor productivity, kg ha^{-1}) and NAE (nitrogen agronomic efficiency, kg ha^{-1}) through a boxplot and a split-half violin plot of the density. NUE values annotated with *, **, or *** are significantly different at $P < 0.1$, $P < 0.05$, or $P < 0.01$, respectively. **b–d** Plots for the average NAE changes in the baseline period (1961–2020) and future period (2021–2100) under the SSP245 and SSP585 scenarios. The solid lines are the mean response curves based on a 5-year moving average.



wheat yields across the major regions in China; (iv) relied on historical weather data from the past 60 years (1961–2020) and forecasted weather data for the next 80 years (2021–2100) (Supplementary Figs. 4–6, Supplementary Table 4); and (v) employed the Global Yield Gap Atlas (GYGA), a bottom-up scaling protocol that was validated for its capacity to reproduce crop performance across large climate variations^{57–59}.

This study explored whether agronomic practices could enhance productivity, narrow yield gaps, improve resource utilization efficiency, and alleviate climate change impacts in winter wheat production in China through a combined approach of field experiments and crop model simulations. First, the simulated national average yields of winter wheat at different levels (YP: 10.3 t ha⁻¹; HYP: 7.5 kg ha⁻¹; HEP: 7.0 kg ha⁻¹; FP:

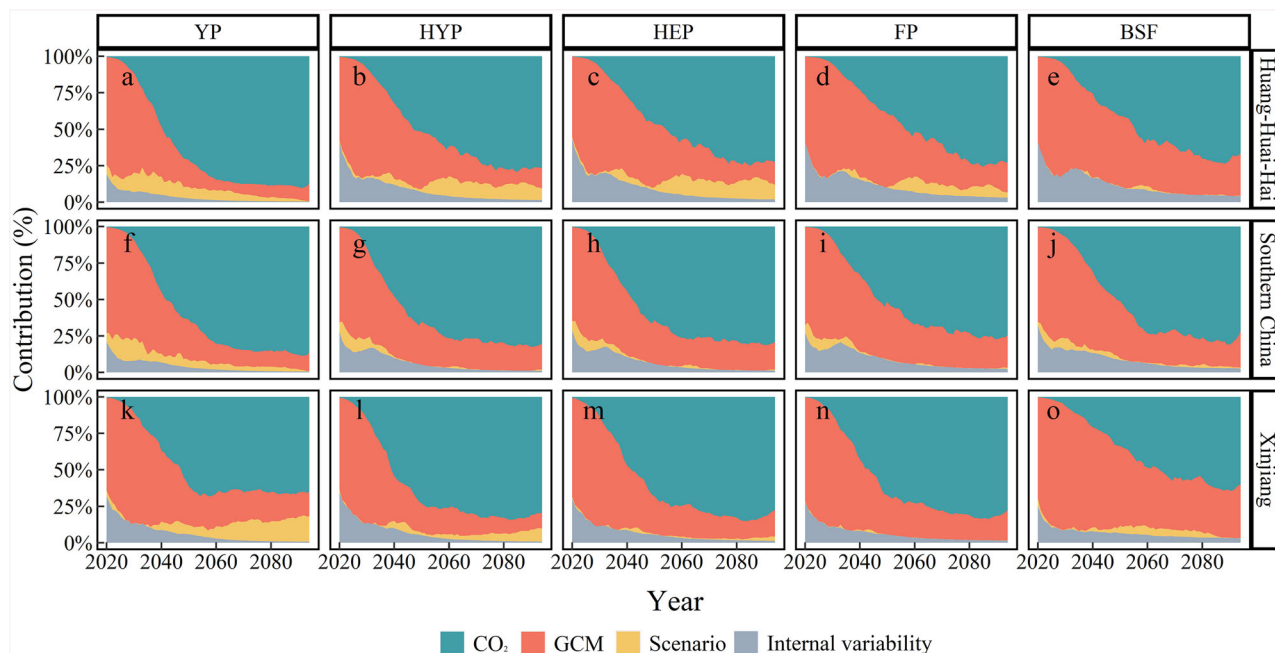


Fig. 10 | Contributions to the uncertainties (%) in projected per-unit yields of winter wheat in the future period of 2021–2100 at five agronomic practices levels in the three main producing regions of China. a–e The Hunag-Huai-Hai region: contributions for the yield levels of YP Yield potential, HYP high-yield practice, HEP High-efficiency practice, FP Farmer practice, BSF Basic soil fertility;

f–j Southern China region: contributions for the same yield levels as (a–e); **k–o** Xinjiang region: contributions for the same yield levels as (a–e). Green, red, yellow, and gray colors represent the changes of uncertainty contributions by CO₂ concentrations, global climate models (GCMs), greenhouse gas emission scenarios, and internal variability, respectively.

6.6 kg ha⁻¹; BSF: 4.5 kg ha⁻¹) in this study differed from previous regional yield assessments, particularly when compared to the national winter wheat yield potential simulated with the APSIM model (8.1 kg ha⁻¹)⁶⁰ and the national yield potential estimated from historical record-high yields (9.0 t ha⁻¹)⁶¹. This finding indicated that the previous conclusions often underestimated the potential yield levels of winter wheat in China^{62–65}. Additionally, this study simulated winter wheat yields at the “HEP” and the “BSF” yield levels under different agronomic practices. However, due to the lack of site-specific experimental data for different agronomic practices, previous studies primarily focused on crop yield gaps related to water-limited and farmer-attainable yields^{62,66–68}. Nevertheless, in the actual winter wheat cultivation systems in China, rainfall was the primary water source in the Southern China region, but besides irrigation, N fertilizer was also an essential measure to increase winter wheat yield in the Huang-Huai-Hai and Xinjiang regions^{19,69}. Therefore, this study combined field experiments with various agronomic practices with crop growth simulation models to assess the potential of different management strategies in narrowing the yield gap of winter wheat, such as irrigation, fertilization, sowing dates, and planting densities. Thus, the approach of yield gap analysis in this study surpassed the relevant studies that examined yield gaps solely based on statistical yields or rain-fed yields.

This study demonstrated that the national yield at “YP” level was about 21% higher than at the “HYP” level (Fig. 6d), which indicated that even when winter wheat approached the maximum achievable yield, there was still room for further yield improvement in the future. In other words, farmers could increase winter wheat yields by further increasing agricultural inputs, particularly by improving irrigation and fertilization practices to ensure an adequate supply of nutrients and water throughout the growing season and to avoid abiotic stress on crop growth. However, different agronomic practices had various degrees of potential to narrow winter wheat yield gaps, and there were great spatial variations both in actual yields and the potential yields under different agronomic practices across China. For instance, in some areas of Xinjiang and the Huang-Huai-Hai regions, there was an obvious upward trend in winter wheat yield over the past 60 years, particularly at the “HYP” and “YP” levels. This could be attributed to

two crucial meteorological factors influencing winter wheat yield under sufficient water and nitrogen conditions, namely solar radiation and temperature. Since the north-high-latitude regions have experienced a faster warming trend globally⁷⁰, winter wheat production in these regions may probably benefit from the future climate change. Jägermeyr et al.⁷¹ showed that global wheat production exhibited a distinct geographical gradient over the past few decades, with a significant increase in winter wheat yields observed in the North China Plain, which was consistent with the results at several yield levels in this study.

In this study, based on combinations of different global climate models (GCMs), climate scenarios, and CO₂ levels, we investigated the spatio-temporal variations in China’s winter wheat yields under future climate change (Supplementary Figs. 8, 9). The predictions of winter wheat yields indicated an overall increasing trend, attributable to the higher temperatures, increased rainfall, and elevated CO₂ concentrations during future winter wheat growing seasons^{71,72}. Xiao et al.⁷³ reported a 7.7%–12.0% increase in wheat yield in the North China Plain under CMIP5 emission scenarios. In this study, winter wheat yield at the “FP” level was predicted to increase by 19.4–44.2% under CMIP6 scenarios. The results indicated that winter wheat productivity under CMIP6 scenarios had a more remarkable improvement than the CMIP5 scenarios, which was also consistent with the result of another study⁷¹.

Distribution and potential for narrowing yield gaps in China

Yield gaps of winter wheat were estimated in many countries worldwide. Generally, the winter wheat yield gap between rainfed and irrigated fields was about 34%⁷⁴. In economically developed countries (e.g., Australia and Germany), wheat yield gaps between rainfed potential yield and farmer’s actual yield ranged from 1.0 to 2.0 t ha⁻¹^{75–78}. However, in major wheat-producing countries in Sub-Saharan Africa (e.g., Tanzania, Kenya, and Ethiopia), yield gaps could reach about 5.8 t ha⁻¹⁷⁹ (www.yieldgap.org). The lower wheat yield gaps in developed countries could be attributed to implementing effective agronomic practices, such as optimal N fertilization in suitable environments^{75,80}. On the other hand, the high yield gaps in developing countries were mainly due to resource shortages, backward

agronomic practices, and smallholder production systems^{81,82}. This study reveals that although the wheat yield gap in China ranks low globally, there remains significant potential to reduce it through scientific advancements, such as improved water and nitrogen management and optimized planting techniques, including sowing adjustments.

Compared with the previous approaches of crop yield gap analysis based on potential yield, rainfed yield, and actual yield, it could provide a more comprehensive and insightful understanding of the underlying causes of yield gaps by incorporating additional crop yield levels. The yield gap analysis based on expanded yield levels can offer a more intuitive reflection of the internal factors shaping yield gaps and served as a valuable reference for devising specific strategies to reduce yield gaps. For instance, in Xinjiang regions, YG-3 was dramatically higher than the other regions (Fig. 7, Supplementary Fig. 11), which indicated that winter wheat yield was very low at the “BSF” level and substantial increase in winter wheat productivity could be achieved by farmers through agronomic practice improvement. This was because the Xinjiang region is a typical arid region in China, characterized by severe water scarcity. Under SSP245 and SSP585 scenarios, the yield gap of YG-3 would increase further. In Xinjiang, wheat cultivation and irrigation mainly occur in spring and summer. Therefore, increasing future droughts in the spring and summer seasons may further enhance the water irrigation requirements for wheat growth in Xinjiang region^{83,84}. The yield gap of YG-2 in Southern China consistently outperformed the other regions under all conditions, indicating a remarkable yield gap between wheat production at the “FP” and the “HEP” levels. This was because improved agronomic practices could enhance resource use efficiency while maintaining crop yield in this region, which was also supported by some previous studies in this region^{63,85,86}. Furthermore, the national yield gap of YG-0 would continuously increase in the future, particularly under the SSP585 scenario in 2061–2100, where YG-0 would exhibit an obvious rise compared with the baseline period of 1961–2020. Since the north-high-latitude regions experienced a faster warming trend in the world, wheat production in Xinjiang and the Huang-Huai-Hai regions would benefit from the future climate (Fig. 6)⁷⁰.

The projection results through the ensemble of multiple GCMs and climate scenarios showed that the variation in yield gaps was not obvious in the 2040 s (2021–2060), but it became greater in the 2080 s (2061–2100) (Supplementary Fig. 12). The range of yield gap changes increased with the climatic vacillation, in other words the projected yield gaps under SSP585 were greater than those under SSP245, while the projected yield gaps in the 2080 s were greater than in the 2040 s. This was consistent with several previous predictions of crop yields in China^{47,73,87,88}. Thus, under future climate conditions, switching from current agronomic practices to “HEP” and “HYP” practices could dramatically increase winter wheat yields (Supplementary Fig. 12). China’s total wheat planting area was about 21.64×10^6 ha in 2020⁸⁹. If the yield gap could be narrowed, the national winter wheat yield would increase by $5.96\text{--}11.92 \times 10^6$ t year⁻¹ without expanding the current winter wheat planting area in the future, which would undoubtedly greatly contribute to world food security.

Suggestions for optimization of agronomic practices

In addition, excessive chemical fertilizer use was frequently observed among smallholders in the intensive crop production systems in China⁹⁰. Unreasonable application of chemical fertilizers resulted in severe agricultural pollution, which necessitated effective policy measures to address the environmental problems caused by N fertilizer. Actually, China has implemented serious policies to reduce N fertilizer application, as evidenced by the national agricultural N application rate exhibited zero growth in 2017⁸⁹. However, simply reducing N fertilizer use across all regions may harm food security. This study found considerable variations in nitrogen use efficiency (NUE), which was represented by PFP (partial factor productivity) and NAE (nitrogen agronomic efficiency), in the three main winter-wheat producing regions of China (Fig. 9), with the Huang-Huai-Hai region having the greatest potential for improving NUE. Studies on water and fertilizer practices in this region also demonstrated that

improving agronomic practices could dramatically enhance NUE while maintaining winter wheat yields^{91–93}. However, it was noteworthy that both PFP and NAE of winter wheat had the highest values at the “FP” level and the lowest values at the “HYP” level in the Xinjiang region. Winter wheat was grown under a condition of high radiation, low temperature, and limited rainfall in the Xinjiang region, resulting in low “BSF” yield (Fig. 6c)^{49,60}. Therefore, irrigation was required in the growing seasons to enhance wheat production (Supplementary Fig. 1). Although increasing N application could boost wheat yield, water availability posed a greater threat to wheat yield. Consequently, the NUE continuously declined despite increased yield. Thus, future improvements in agronomic practices should focus on enhancing water utilization efficiency (WUE), reducing soil evaporation, and optimizing light and temperature resource use to optimize the agronomic practices in Xinjiang region. Attention should be paid to improving the frequency and amount of drip irrigation, applying plastic-film mulching, and adjusting sowing date and density^{50,94–96}.

In contrast, the findings about WUE in winter wheat production differed from those of NUE in this study. The WUE_u did not show a gradient difference in its geographical distribution (Fig. 8), and this was also the case in the future predictions (Supplementary Fig. 17a–b). This was probably due to the design of the agronomic practices at the experimental sites in this study. Due to the severe droughts and limited water resources in the Xinjiang region, an advanced drip irrigation technique with high irrigation rates was adopted for winter wheat cultivation to ensure normal growth (Supplementary Table 1 and Supplementary Fig. 1)^{50,96}. In contrast, winter wheat production mainly relied on rainfall in Southern China due to abundant water resources. This situation led to similar water inputs in different agronomic practices, which could result in small differences in WUE across different winter-wheat producing regions in China. This reflected the actual local farming conditions. Future predictions indicated that the WUE_u at the “HEP” and “HYP” levels was significantly higher than at the “FP” level in Southern China. This finding demonstrated that despite of the general absence of irrigation in the growing seasons of winter wheat, improving agronomic practices could still enhance water resource utilization efficiency in Southern China.

We compared the relative changes in NUE and WUE between the “HEP” and “FP” levels, as well as between the “HYP” and “FP” levels (Supplementary Fig. 16). This study demonstrated that improving agronomic practices could narrow either the yield gap or the NUE gap in the Huang-Huai-Hai region. However, it could not simultaneously narrow the two gaps of yield and NUE in this region. This study indicated that increasing the N rate could effectively reduce both yield gaps and efficiency gaps in Southern China. With higher nitrogen application, winter wheat yield increased by approximately 14.6–20.5%, and NAE also increased by more than 20%. Therefore, increasing N fertilizer application could be considered an optimal agronomic practice in this region. In contrast to this region, with high N fertilizer input at the “HEP” and “HYP” levels in Xinjiang region, the yield increased by only about 3.2% and 9.3%, but the NUE decreased by over 20% (Supplementary Fig. 16). Thus, this study demonstrated that if winter wheat yield needed to increase in the Xinjiang region in the future, resource use efficiency should not be disregarded.

The relative changes in NUE and WUE in the 2040 s period were similar to those in the baseline period (1961–2020), but different from the 2080 s period under future climate change in China (Supplementary Fig. 18). With elevated CO₂ concentrations in the SSP585 scenario, improvements in agronomic practices in the 2080s could further reduce the yield and efficiency gaps in winter wheat production. This would alleviate the contradiction between resource use efficiency and agricultural yield in future winter wheat production in China (Supplementary Fig. 18a, b). This study demonstrated that future wheat production in China would increase with the agronomic practices at the “HEP” level, while the utilization efficiency of water and N resources would be dramatically improved compared to the high-input level of “HYP”. Thus, due to the obvious environmental variations across different regions in China, different winter wheat producing regions in China should improve their agronomic practices according

to their own development needs. For instance, the regions with abundant water resources or lower fertilizer costs (e.g., the Huang-Huai-Hai region) could prioritize narrowing yield gaps and pursuing yield potential. However, if the objective was to reduce economic costs and minimize the ecological impacts of N fertilizers while maintaining current wheat yields, improving agronomic practices could enhance fertilizer use efficiency and narrow the efficiency gap. In Southern China, efficient agronomic practices could simultaneously narrow yield gaps and improve resource use efficiency, and therefore, such practices should be encouraged. In contrast, in Xinjiang, agronomic practices should be optimized according to the specific needs, as yield increase would inevitably reduce resource use efficiency in the region. In conclusion, improving agronomic practices could reduce yield disparities or resource utilization gaps in all winter wheat-producing regions of China. Furthermore, this conclusion remained valid in the context of future climate change in China.

Uncertainties in winter wheat yield projections

By analyzing the uncertainties in the projections of winter wheat yields under future climate change, this study elucidated the main factors underlying future variations in winter wheat yields. In the initial stage of the 2021–2100 period, the global climate models (GCMs) emerged as the primary source of uncertainty in the predictions of winter wheat yields in China, followed by internal variability and future greenhouse gas emission scenarios. Actually, Jiang et al.^{47,87} also found that GCMs were the major uncertainty contributor in future predictions of winter wheat yields in the Loess Plateau (a part of the Huang-Huai-Hai region) of China. However, this study found that the projection uncertainties contributed by different factors varied over time. Uncertainty contributions from GCMs and internal variability gradually decreased over time, while those from CO₂ concentration and climate scenarios increased. Especially in the initial several decades, the uncertainty contributions from the scenario could be neglected. However, at the potential yield levels nationwide and at most yield levels in the Huang-Huai-Hai region, scenario uncertainty gradually increased. This could be explained by the remarkable influences of global warming and increased radiative forcing on the yield potential and production of winter wheat after 2050. Lu et al.⁹⁷ also demonstrated that the scenarios would gradually exceed the internal variability in contributions to projection uncertainties and become the primary uncertainty source after 2050. Notably, the impacts of CO₂ concentrations on winter wheat production in China would gradually increase and become the largest uncertainty source after 2050. Based on the projections of future yield levels, it was found that future increases in greenhouse gases would positively affect the winter wheat yield in China, which was consistent with the findings of numerous related studies in the past^{71,73,87}. Furthermore, it was found that improving current agronomic practices would enhance the positive effects of CO₂ concentration, thereby providing even greater benefits to winter wheat production in China.

Future recommendations for efficient agronomic practices

Previous studies typically focused on simulations of rainfed systems and temperature-radiation potentials, lacking detailed classifications of yield gap types. In contrast, this study offered a practical and targeted solution to address yield gaps, specifically proposing the implementation of more effective agronomic practices tailored to different regions. There were certain uncertainties in the model simulations in this study, primarily due to the errors in soil and weather data, the impacts of extreme climate events, and the interference of non-climatic factors such as pests and diseases. Thus, future researches should increase model simulation accuracy by using higher-resolution data or through data assimilation methods to improve prediction reliability^{3,98}. However, the main objective of this study was to analyze, through upscaling simulations and future predictions, whether agronomic practices could serve as an effective approach to address the growing challenges of climate change. By conducting agronomic trials at sites and integrating climate change predictions into the model, this research provided concrete strategies for

narrowing yield gaps. Additionally, uncertainty analysis supported the conclusion that optimizing agronomic practices was the most effective way for China's wheat production to adapt to future warming and increased CO₂. This study proposed efficient agronomic practices as a feasible solution to address the potential opportunities and challenges in future agricultural sustainability. However, actual implementation of these practices will require further investigation into the social and economic conditions in China, considering the great regional variations in socio-economic factors, infrastructure limitations, cost constraints, cultural preferences, and knowledge gaps. This may necessitate government support through subsidies for precision irrigation or technical guidance for farmers in underdeveloped areas in China.

Methods

Field experiments and levels of agronomic managements

The field experiments in this study were based on a project in the 'Five-Year Plan' for Agriculture by the Chinese government. The project had several objectives: the first was to explore the distribution of winter wheat yield gaps across the whole country; and the second was to investigate the potential for narrowing these yield gaps and enhancing water and nutrient use efficiency through optimized management practices in wheat production in China. A distinctive feature of the project was the establishment of experimental sites across the country, where continuous multi-year trials were conducted. This study mainly focused on the potential for increasing winter wheat yields in China in the future. A total of five different yield levels were set for crop model simulations (Figs. 1a and 2), but only four levels (except for the 'Potential yield' level) were tested at the experimental sites in the three major winter-wheat producing regions (i.e., Xinjiang, Huang-Huai-Hai, and Southern China) in China. A total of 22 different sites were selected for three-year (2017–2019) field experiments (Fig. 3b) across China. According to the project requirements, the selected sites were chosen from both traditional wheat growing regions and high-density wheat cultivation areas in China. These sites have a history of wheat cultivation more than ten years, with a large number of local farmers engaged in wheat farming in the surrounding areas. A comparison of the wheat planting density maps demonstrated that the selection of these sites could meet the specified criteria (Fig. 3). At each site four different levels of agronomic management practices (i.e., BSF, FP, HEP, and HYP; Fig. 1a) were implemented for local winter wheat production. The differences among the agronomic practice levels were reflected in the differences in irrigation rate, N fertilizer rate, sowing date, and seeding density. Variations also existed in the irrigation and fertilization frequency (Supplementary Table 1 and Supplementary Fig. 1).

Previous yield gap studies usually divided crop yield into different levels, thus resulting in different definitions of the yield gap. This study combined the previous yield-gap assessment protocols and defined five different yield levels were first defined, and then the yield gaps were defined as the differences between two adjacent yield levels (Fig. 1a). The yield levels of 'Yield potential' (YP) referred to the maximum yield simulated by crop model under the conditions without nutrient deficiency, pests, or diseases^{5,99}. Corresponding to the four levels of agronomic management, there were also four different levels of yields, namely 'High-yield practice' (HYP), 'High-efficiency practice' (HEP), 'Farmer practice' (FP), and 'Basic soil fertility' (BSF).

More specifically, the agronomic management level of 'Farmer practice' (FP) referred to the field management measures of local farmers, representing the typical local agricultural practice. A total of 2–5 villages were randomly selected in the county where the experimental sites were located, and several farmers were randomly selected in each village for interview, mainly about their management practices for winter wheat production. The 'High-efficiency practice' (HEP) level was the optimized local agronomic practices by researchers based on previous cultivation experiments to ensure higher crop yields and higher resource utilization efficiency. The optimized management strategies included appropriate planting density and row spacing, suitable N fertilizer amount and

application schedule, and supplementary irrigation when needed^{100–102}. The ‘High-yield practice’ (HYP) level referred to sufficient irrigation and N fertilizer for the high-yield and high-efficiency management measures, ensuring that crop plants were not subject to water and N stresses in growth, and achieving the highest yield that could be obtained at the experimental sites. And the ‘Basic soil fertility’ (BSF) level referred to the final yield that was obtained without any irrigation or fertilization during the whole growing season of winter wheat.

Protocols for yield gap assessment and spatial upscaling

In this study, we followed the protocols established by the Global Yield Gap Atlas (GYGA; www.yieldgap.org) to estimate the yield gaps of winter wheat. The GYGA utilized the primary, location-specific data to the extent possible and a robust upscaling framework to estimate yield gaps at larger levels of spatial aggregation, such as climate zones (CZ), regions, and national scales. The GYGA protocols were based on a matrix of three categorical variables (growing degree days, aridity index, and temperature seasonality) to delineate the climate zones for harvested areas of food crops^{58,103}. Buffer zones of the reference weather stations (RWS) in each region were selected following the protocol described in GYGA for winter wheat production^{23,59,104}. In this protocol, the climate zone map was superposed on a digital map of spatial distributions of winter wheat (with a grid-cell resolution of 10 km × 10 km)¹⁰⁵ to identify the weather stations located in areas with the greatest density of wheat production. Then circles with 100-km radius were drawn as the buffer zone to surround all of the weather stations. Previous research indicated that increasing the number of reference weather stations to cover more crop growing areas actually did not improve the estimates of yield gaps at the regional level⁷⁸. Thus, it was rational to select the buffer zones from big to small in each region according to their covered harvested wheat areas until the total harvested area became greater than 50% of the buffer zones. Following this protocol, a total of 82 reference weather stations (RWS), which covered about 60% of the national harvested wheat areas, were selected with their individual buffer zones. The 82 reference weather stations were located in 26 climate zones, covering about 89% of the national wheat production areas (Fig. 3b). More details about the locations of selected reference weather stations and the dominant planting cultivars in each RWS buffer zone were provided in Supplementary Table 1.

The selected reference weather stations were then grouped into three main winter-wheat producing regions (i.e., Huang-Huai-Hai region, Southern China region, and Xinjiang region) in China according to the climate zones and their different cultivation systems (Fig. 3a). The Huang-Huai-Hai region mainly adopted the wheat-maize rotation system, the Southern China region mainly adopted the rice-wheat rotation system, and the Xinjiang region implemented a very specific dryland agricultural system with drip irrigation due to scarce precipitation. To estimate wheat yields and yield gaps in different agricultural climate zones and the three main producing regions, we first used the harvested wheat areas within RWS buffer zones as the weights for spatial upscaling (Eq. 1). Then, we used the harvested wheat areas in the climate zones in each main producing region as the weights for spatial upscaling (Eq. 2).

$$Y_{\text{climatezone}} = \frac{\sum_{i=1}^q Y_{\text{station}_i} \times \text{Area}_{\text{RWSbufferzone}_i}}{\sum_{i=1}^q \text{Area}_{\text{RWSbufferzone}_i}} \quad (1)$$

where $Y_{\text{climatezone}}$ is the crop yield at climate zone level; q is the number of reference weather stations within the climate zone; and $\text{Area}_{\text{RWSbufferzone}_i}$ is the harvested crop area in the buffer zone of i -th reference weather station.

$$Y_{\text{area}} = \frac{\sum_{i=1}^s Y_{\text{climatezone}_i} \times \text{Area}_{\text{climatezone}_i}}{\sum_{i=1}^s \text{Area}_{\text{climatezone}_i}} \quad (2)$$

where Y_{area} is the crop yield in different main winter-wheat producing regions; s is the number of climate zones in each winter-wheat producing

region; and $\text{Area}_{\text{climatezone}_i}$ is the harvested crop area in the i th climate zone in each winter-wheat producing region.

Weather and soil data sources

Long-term measured daily weather data were crucial for robust simulation of the phenology dates and yields of winter wheat. The meteorological data required for model simulation included maximum and minimum temperature, wind speed, and solar radiation. Daily weather data were obtained for all weather variables (except for solar radiation) in 60 historical years (1961–2020) from the National Meteorological Information Center (<http://data.cma.cn/>) of China Meteorological Administration for the selected representative weather stations and the experimental sites. Following previous research, the solar radiation data were calculated based on daily sunshine hours in the meteorological data¹⁰⁶. The weather data used in this study underwent quality control methods and were widely applied in past relevant studies.

Soil properties could affect the simulation accuracy of winter wheat yield, as they generally did not change over time but could vary greatly among different regions. Soil water-holding properties, which were related to the soil water balance in the experimental sites and the reference weather stations, were obtained from the Chinese soil hydrographic dataset (<http://www.nesdc.org.cn/>)¹⁰⁷. Other soil properties, including ammonium N, nitrate N, bulk density, organic carbon, and pH at different soil depths, were measured and calculated at the experimental sites. Meanwhile, these same soil properties of the reference weather stations were obtained from the Chinese soil hydrographic dataset and the HWDS (Harmonized World Soil Database version 1.1) dataset¹⁰⁸.

Crop model simulations of different levels of winter wheat yields

Crop growth models can simulate wheat growth, development, and yield by considering the interaction of environment, genetic, and management. Five wheat yield levels were simulated with the DSSAT-CERES-wheat V4.7 model based on the actual crop management practices in the field experiments¹⁰⁹, measured daily weather data, soil characteristics, and genetic parameters of the representative wheat varieties. This model has been well validated in field experiments conducted in various environments and extensively used to simulate yield levels in various wheat cropping systems in the world^{47,110–112}. To compare the simulated results with the actual observations at the sites, we simulated winter wheat growth for each yield level across all of the 22 experimental sites involved.

The experiments were conducted for three continuous years from 2017–2019, with 19 different wheat varieties involved. More specifically, two different wheat varieties were planted in the Huang-Huai-Hai region and three in the Xinjiang region, and the same varieties were planted at the same sites in these two regions for three years. However, there were a total of 14 different wheat varieties involved in the experiments in the Southern China region because different varieties were planted in different years, even at the same experimental site. Thus, wheat varieties in Xinjiang and the Huang-Huai-Hai regions were generally stable, while the 14 wheat varieties in the Southern China region were grouped and represented by three sets of genetic parameters according to their administrative regions. Additionally, crop model simulations with the regional representative wheat varieties could also ensure the accuracy of regional simulations of winter wheat yields¹¹³.

First, the genetic parameters of different wheat varieties were evaluated through the least square method with the R language. For each winter wheat variety, model calibration was conducted based on the experimental data from one site-year experiment, and model validation was performed with the data from other site-year(s). These two sets of experimental data were independent. The experimental observation data included yields, phenology dates (anthesis and maturity), fertilizer partial factor productivity (FPF), and nitrogen agronomic efficiency (NAE) of winter wheat. Model calibrations were conducted in different regions and at various yield levels, respectively (Supplementary Figs. 4–6). Degrees of association and agreement between simulated and observed variables were assessed by the coefficient of

determination (R^2 ; Eq. 3), root mean square error (RMSE; Eq. 4), and RMSE expressed as a percentage of the observed mean (NRMSE; Eq. 5).

$$R^2 = \left(\frac{n(\sum xy) - (\sum x)(\sum y)}{[n \sum x^2 - (\sum x)^2][n \sum y^2 - (\sum y)^2]} \right)^2 \quad (3)$$

$$RMSE = \left[\left(\sum (x - y)^2 / n \right) \right]^{0.5} \quad (4)$$

$$NRMSE = \left[\left(\sum (x - y)^2 / n \right) \right]^{0.5} / M_{mean} \times 100\% \quad (5)$$

where x and y represent the simulated and observed variable values, and n represents the number of paired values. R^2 close to 1 and RMSE/NRMSE close to 0 indicate a good agreement between the model-simulated and field-observed values.

Although there were disparities between different yield levels, the simulated yields were in close agreement with the observed yields after model calibration. The RMSE value was less than 1.0 t ha⁻¹ in the three main wheat-producing regions. The NRMSE was about 14.2% in the Southern China region but was less than 5% in Xinjiang region (Supplementary Fig. 4). The results of model validations at different yield levels showed that the RMSE at the ‘Farmer practice’ level was higher than the other three levels, due to higher simulated yields than the actual yields at the experimental sites. However, the R^2 of all simulation results was greater than 0.5 and was concentrated along the 1:1 lines (Supplementary Fig. 5). The model validation results of wheat phenology dates (anthesis and maturity dates) were similar to the yields. The RMSE values of anthesis and maturity dates were 2.1–3.5 d and 3.0–4.0 d, or 0.9%–2.4% and 1.4%–1.7% of the average observation dates, respectively. In summary, the reasonable agreement between the observed and simulated yields and phenology dates of winter wheat confirmed that the calibrated CERES-wheat model was robust in reproducing the different yield levels across a wide range of climates and wheat cropping systems in China. We then conducted model simulations at each selected reference weather station by referring to the genetic parameters of the representative regional wheat variety and the agronomic practices in the experimental station that was closest to the reference weather station. In the processes of model calibration and validation at each experimental station, four wheat yield levels were simulated because actual measurements were available for comparisons. In addition, the potential yield level was also simulated, resulting in five simulated yield levels according to the yield gaps of winter wheat defined previously (Fig. 1).

Winter wheat yield projections under future climate scenarios

In this study, we assessed the impacts of future climate changes on yield gaps and resource use efficiency of winter wheat by projecting the yields at different production levels in future periods of 2021–2100 under two different scenarios of SSP245 and SSP585 based on the Coupled Model Intercomparison Project phase (CMIP6). The Mann-Kendall test was used to perform trend analysis for winter wheat yields in the baseline and future periods^{114,115}. Moreover, the response of the crop to atmospheric CO₂ concentration was considered and fitted for the two scenarios based on the projection data from the SSP database (Eqs. 6 and 7)¹¹⁶. Thus, we could evaluate the effects of stable and changing CO₂ levels on wheat production under each scenario. Future climate in periods of 2021–2060 and 2061–2100 of each reference weather station were obtained from a total 27 different global climate models (GCMs; Supplementary Table. 4). The statistical downscaling model Nwai-WG, which was developed by Liu and Zuo¹¹⁷, was used to downscale the GCM monthly gridded data to daily climate data for each of the selected reference weather stations. This statistical

downscaling model were widely used and evaluated in China and Australia^{87,87,118}.

$$[CO_2]_{year} = 62.044 + \frac{34.002 - 3.8702 \times y}{0.24423 - 1.1542 \times y^{2.0001}} + 0.028057 \times (y - 1900)^2 + 0.00026827 \times (y - 1960)^3 - 9.2751 \times 10^{-7} \times (y - 1910)^4 - 2.2448 \times (y - 2030) \quad (6)$$

$$[CO_2]_{year} = 757.44 + \frac{84.938 - 1537 \times y}{0.2011 - 38289 \times y^{-0.4532}} + 2.4712 \times 10^{-4} \times (y + 15)^2 + 1.9299 \times 10^{-5} \times (y - 1937)^3 + 5.1137 \times 10^{-7} \times (y - 1910)^4 \quad (7)$$

Calculations of water and nitrogen fertilizer use efficiencies

Nitrogen use efficiency (NUE) is a key indicator to study nitrogen cycles and inform nitrogen management, which measures the efficiency and potential environmental impacts of nitrogen use in crop production^{19,20,28,119,120}. In this study, we used the fertilizer partial factor productivity (FPF, kg wheat grain per kg fertilizer applied; Eq. 8) and nitrogen agronomic efficiency (NAE, kg wheat grain per kg fertilizer applied; Eq. 9) as the measures of fertilizer use efficiency since both of these two indicators could reflect the balance between indigenous N supply and applied N fertilizer.

$$FPF = G_N / F_N \quad (8)$$

$$NAE = (G_N - G_{Basic\ soil}) / F_N \quad (9)$$

where G_N is the grain yield with N fertilizer application (kg ha⁻¹); $G_{Basic\ soil}$ is the crop yield without N application (kg ha⁻¹); F_N is the amount of N fertilizer applied (kg ha⁻¹).

Howell¹²¹ defined crop water use efficiency (WUE) for yield levels as the income of crop yield obtained per unit of water input¹²². In this study, we selected three widely used indicators for crop water use efficiency analysis and evaluation, including water productivity (WP, kg m⁻³; Eq. 10), broad water use efficiency (WUE_w, kg m⁻³; Eq. 11), and irrigation water use efficiency (WUE_i, kg m⁻³; Eq. 12). This was because these indicators had varying calculation methods, physical meanings, and application contexts.

$$WP = Y / (10 \times ET) \quad (10)$$

$$WUE_w = Y / [10 \times (P + I)] \quad (11)$$

$$WUE_i = Y / (10 \times I) \quad (12)$$

where Y is wheat grain yield at different yield levels, kg ha⁻¹; ET is total season evapotranspiration, mm, which was calculated by the soil-plant-atmosphere interface module in the DSSAT model; P is the amount of precipitation during the growing season of winter wheat, mm; I is the amount of irrigation during the growing season of winter wheat, mm. After calculating water and nitrogen use efficiency, analysis of variance (ANOVA) was conducted to compare the significant differences between different agronomic practices. The changes in N rate, irrigation rate, NAE, WUE_w, and yield under the ‘High-efficiency practice’ and ‘High-yield practice’ levels were calculated and compared with those under the ‘Farm practice’ level. The relative changes were calculated using a specific method.

$$Relative\ Change = \frac{Treatment\ Value - Control\ Value}{Control\ Value \times 100\%} \quad (13)$$

where the treatment value is the variable values under the ‘High-efficiency practice’ (HEP) and ‘High-yield practice’ (HYP) levels; and the control value is the values of the same variables under the ‘Farm practice’ (FP) level.

Quantification of the uncertainties in winter wheat yield projections

Before separating the uncertainties in the projections of winter wheat yield, a ten-year moving average was used to smooth the time series since winter wheat yields had a large interannual variability. The HS09 method was developed to characterize the contributions by the internal variability, model uncertainty and scenario uncertainty to CMIP6 GCM projections¹²³, which was proven to be an effective method for distinct sources of uncertainty in climate predictions^{54,55,124,125}. In this study, the HS09 method was also used to separate the projection uncertainties contributed by CO₂ concentrations, models, scenarios, and internal variability. The main procedures of the HS09 method were summarized as follows.

(1) Each individual prediction variable (x) was fitted by a fourth-order polynomial in years of 2020–2100, based on the smooth fit (X) for each GCM (g), scenario (s), CO₂ concentration change (c), and year (t) (Eq. 14).

$$x_{g,s,c,t} = X_{g,s,c,t} + \varepsilon_{g,s,c,t} \quad (14)$$

where $X_{g,s,c,t}$ is the smooth fit for each GCM, scenario, year, and CO₂ concentration change; $\varepsilon_{g,s,c,t}$ is the residual of the smooth fit.

(2) The projection uncertainty contributed by GCMs (M_t) was expressed by the variance across the global climate models (Eq. 15).

$$M_t = \frac{\sum_{s,c=1}^{N_s+N_c} \text{Var}_g(X_{f,g,s,c,t})}{N_s + N_c} \quad (15)$$

where N_s is the number of scenarios, $N_s = 2$; N_c is the number of CO₂ conditions, $N_c = 2$.

(3) The projection uncertainty contributed by scenario (S_t) was expressed by the variance of the mean values of each GCM under each scenario (Eq. 16).

$$S_t = \text{var}_s \left(\frac{\sum_{g=1}^{N_g} X_{g,s,c,t}}{N_g} \right) \quad (16)$$

where N_g is the total number of GCMs for each scenario and CO₂ concentration changing, $N_g = 27$.

(4) The projection uncertainty caused by CO₂ concentration changing (C_t) was calculated by the variance of GCMs mean for each CO₂ concentration changing in t -th year (Eq. 17).

$$C_t = \text{Var}_c \left(\frac{\sum_{g=1}^{N_g} X_{g,s,c,t}}{N_g} \right) \quad (17)$$

(5) The internal variability (Int) for each GCM was calculated by the variances of scenario, CO₂ concentration changing, and time, which were estimated independently of scenario, CO₂ concentration changing, and lead time (Eq. 18).

$$Int = \frac{\sum_{g=1}^{N_g} \text{Var}_{c,s,t}(\varepsilon_{g,c,s,t})}{N_g} \quad (18)$$

(6) The total uncertainty (T_t) were calculated by Eq. 19.

$$T_t = M_t + S_t + C_t + Int \quad (19)$$

The contributions of internal variability, models, and scenarios to the total uncertainties in winter wheat yield projections were all expressed as percentage.

Reporting summary

Further information on research design is available in the Nature Portfolio Reporting Summary linked to this article.

Data availability

The historical meteorological data can be obtained at <http://data.cma.cn/>. The CMIP6 data can be accessed at <https://esgf-node.lnl.gov/projects/cmip6/>. The soil properties can be accessed at <https://www.nesdc.org.cn/>, and crop model emulators can be found at <https://dssat.net/>. The datasets used in this study have been deposited in the public data repository at <https://doi.org/10.5281/zenodo.15140289>.

Code availability

The scripts for data analyses are available at <https://doi.org/10.5281/zenodo.15140289>.

Received: 12 December 2024; Accepted: 7 April 2025;

Published online: 16 April 2025

References

1. FAOSTAT. *Production Data*. (FAO, accessed 1 April 2023).
2. NBSC. *National Bureau of Statistics of China, China Statistical Yearbook*. (China Statistic Press, Beijing, China, 1980–2020).
3. Kheir, A. M. S. et al. Developing automated machine learning approach for fast and robust crop yield prediction using a fusion of remote sensing, soil, and weather dataset. *Environ. Res. Commun.* **6**, 41005 (2024).
4. Mueller, N. D. et al. Closing yield gaps through nutrient and water management. *Nature* **490**, 254–257 (2012).
5. Lobell, D. B., Cassman, K. G. & Field, C. B. Crop yield gaps: their importance, magnitudes, and causes. *Annu. Rev. Env. Resour.* **34**, 179–204 (2009).
6. Lobell, D. B. et al. The critical role of extreme heat for maize production in the United States. *Nat. Clim. Change* **3**, 497–501 (2013).
7. Lesk, C., Coffel, E. & Horton, R. Net benefits to US soy and maize yields from intensifying hourly rainfall. *Nat. Clim. Change* **10**, 819–822 (2020).
8. Li, Y., Guan, K., Schnitkey, G. D., DeLucia, E. & Peng, B. Excessive rainfall leads to maize yield loss of a comparable magnitude to extreme drought in the United States. *Glob. Change Biol.* **25**, 2325–2337 (2019).
9. Qin, X. et al. Wheat yield improvements in China: Past trends and future directions. *Field Crop. Res.* **177**, 117–124 (2015).
10. Xin, Y. & Tao, F. Developing climate-smart agricultural systems in the North China Plain. *Agric. Ecosyst. Environ.* **291**, 106791 (2020).
11. Xiao, L. et al. Spatiotemporal co-optimization of agricultural management practices towards climate-smart crop production. *Nat. Food* **5**, 59–71 (2024).
12. Luo, N. et al. China can be self-sufficient in maize production by 2030 with optimal crop management. *Nat. Commun.* **14**, 2637 (2023).
13. Rizzo, G. et al. Climate and agronomy, not genetics, underpin recent maize yield gains in favorable environments. *Proc. Natl. Acad. Sci.* **119**, e2113629119 (2022).
14. Kheir, A. M. S. et al. Minimizing trade-offs between wheat yield and resource-use efficiency in the Nile Delta – A multi-model analysis. *Field Crop. Res.* **287**, 108638 (2022).
15. Kheir, A. M. S. et al. Impacts of climate change on spatial wheat yield and nutritional values using hybrid machine learning. *Environ. Res. Lett.* **19**, 104049 (2024).
16. Arduini, I., Masoni, A., Ercoli, L. & Mariotti, M. Grain yield, and dry matter and nitrogen accumulation and remobilization in durum wheat as affected by variety and seeding rate. *Eur. J. Agron.* **25**, 309–318 (2006).
17. Chen, S., Zhang, X., Sun, H., Ren, T. & Wang, Y. Effects of winter wheat row spacing on evapotranspiration, grain yield and water use efficiency. *Agr. Water Manag.* **97**, 1126–1132 (2010).
18. Yu, C. et al. Managing nitrogen to restore water quality in China. *Nature* **567**, 516–520 (2019).

19. Cai, S. et al. Optimal nitrogen rate strategy for sustainable rice production in China. *Nature* **615**, 73–79 (2023).
20. Wang, J. et al. Effects of nitrogen application rate under straw incorporation on photosynthesis, productivity and nitrogen use efficiency in winter wheat. *Front. Plant Sci.* **13**, (2022).
21. Dang, P. et al. Effects of different continuous fertilizer managements on soil total nitrogen stocks in China: A meta-analysis. *Pedosphere* **32**, 39–48 (2022).
22. Chen, Y. et al. Crop management based on multi-split topdressing enhances grain yield and nitrogen use efficiency in irrigated rice in China. *Field Crop. Res.* **184**, 50–57 (2015).
23. Chen, X. et al. Integrated soil–crop system management for food security. *Proc. Natl. Acad. Sci.* **108**, 6399–6404 (2011).
24. Zhao, Y., Chen, X. & Lobell, D. B. An approach to understanding persistent yield variation—A case study in North China Plain. *Eur. J. Agron.* **77**, 10–19 (2016).
25. Fan, Y., Wang, C. & Nan, Z. Determining water use efficiency of wheat and cotton: A meta-regression analysis. *Agr. Water Manag.* **199**, 48–60 (2018).
26. Zhang, W. et al. Closing yield gaps in China by empowering smallholder farmers. *Nature* **537**, 671–674 (2016).
27. Zhang, D. et al. Nitrogen application rates need to be reduced for half of the rice paddy fields in China. *Agric. Ecosyst. Environ.* **265**, 8–14 (2018).
28. Quan, Z., Zhang, X., Fang, Y. & Davidson, E. A. Different quantification approaches for nitrogen use efficiency lead to divergent estimates with varying advantages. *Nat. Food* **2**, 241–245 (2021).
29. Lassaletta, L., Einarsson, R. & Quemada, M. Nitrogen use efficiency of tomorrow. *Nat. Food* **4**, 281–282 (2023).
30. Wang, J., Wang, E., Yang, X., Zhang, F. & Yin, H. Increased yield potential of wheat-maize cropping system in the North China Plain by climate change adaptation. *Clim. Change* **113**, 825–840 (2012).
31. Zhang, X., Chen, S., Liu, M., Pei, D. & Sun, H. Improved water use efficiency associated with cultivars and agronomic management in the North China Plain. *Agron. J.* **97**, 783–790 (2005).
32. Sun, H. et al. Effect of precipitation change on water balance and WUE of the winter wheat–summer maize rotation in the North China Plain. *Agr. Water Manag.* **97**, 1139–1145 (2010).
33. Hu, Y., Moiwu, J. P., Yang, Y., Han, S. & Yang, Y. Agricultural water-saving and sustainable groundwater management in Shijiazhuang Irrigation District, North China Plain. *J. Hydrol.* **393**, 219–232 (2010).
34. Zhang, X., Wang, Y., Sun, H., Chen, S. & Shao, L. Optimizing the yield of winter wheat by regulating water consumption during vegetative and reproductive stages under limited water supply. *Irrig. Sci.* **31**, 1103–1112 (2013).
35. Zhang, X. et al. Incorporating root distribution factor to evaluate soil water status for winter wheat. *Agr. Water Manag.* **153**, 32–41 (2015).
36. Zhang, X., Chen, S., Sun, H., Wang, Y. & Shao, L. Water use efficiency and associated traits in winter wheat cultivars in the North China Plain. *Agr. Water Manag.* **97**, 1117–1125 (2010).
37. Sun, B. et al. Agricultural non-point source pollution in China: Causes and Mitigation Measures. *Ambio* **41**, 370–379 (2012).
38. Liu, X. et al. Enhanced nitrogen deposition over China. *Nature* **494**, 459–462 (2013).
39. Guo, J. H. et al. Significant acidification in major Chinese croplands. *Science* **327**, 1008–1010 (2010).
40. Yang, Y. et al. Climate change exacerbates the environmental impacts of agriculture. *Science* **385**, n3747 (2024).
41. Du, Y. et al. A synthetic analysis of the effect of water and nitrogen inputs on wheat yield and water- and nitrogen-use efficiencies in China. *Field Crop. Res.* **265**, 108105 (2021).
42. Rezaei, E. E. et al. Climate change impacts on crop yields. *Nat. Rev. Earth Environ.* **4**, 831–846 (2023).
43. He, M. et al. Long-term appropriate N management can continuously enhance gross N mineralization rates and crop yields in a maize-wheat rotation system. *Biol. Fert. Soils* **59**, 501–511 (2023).
44. Bassu, S. et al. How do various maize crop models vary in their responses to climate change factors?. *Glob. Change Biol.* **20**, 2301–2320 (2014).
45. Sun, S., Yang, X., Lin, X., Sassenrath, G. F. & Li, K. Climate-smart management can further improve winter wheat yield in China. *Agr. Syst.* **162**, 10–18 (2018).
46. Kheir, A. M. S. et al. Integrating APSIM model with machine learning to predict wheat yield spatial distribution. *Agron. J.* **115**, 3188–3196 (2023).
47. Jiang, T. et al. Identifying sources of uncertainty in wheat production projections with consideration of crop climatic suitability under future climate. *Agr. Meteorol.* **319**, 108933 (2022).
48. Rosenzweig, C. et al. Assessing agricultural risks of climate change in the 21st century in a global gridded crop model intercomparison. *Proc. Natl. Acad. Sci.* **111**, 3268–3273 (2014).
49. Li, Q., Chen, Y., Shen, Y., Li, X. & Xu, J. Spatial and temporal trends of climate change in Xinjiang, China. *J. Geogr. Sci.* **21**, 1007–1018 (2011).
50. Rao, F., Abudukeranmu, A., Shi, X., Heerink, N. & Ma, X. Impact of participatory irrigation management on mulched drip irrigation technology adoption in rural Xinjiang, China. *Water Resour. Econ.* **33**, 100170 (2021).
51. Heng, T., He, X., Yang, L., Xu, X. & Feng, Y. Mechanism of saline-alkali land improvement using subsurface pipe and vertical well drainage measures and its response to agricultural soil ecosystem. *Environ. Pollut.* **293**, 118583 (2022).
52. Chen, D., Gao, G., Xu, C., Guo, J. & Ren, G. Comparison of the Thornthwaite method and pan data with the standard Penman-Monteith estimates of reference ET in China. *Clim. Res.* **28**, 123–132 (2005).
53. Wu, D. et al. Analysis of variation in reference evapotranspiration and its driving factors in mainland China from 1960 to 2016. *Environ. Res. Lett.* **16**, 54016 (2021).
54. Chen, X. et al. Projected dry/wet regimes in China using SPEI under four SSP-RCPs based on statistically downscaled CMIP6 data. *Int. J. Climatol.* **42**, 9357–9384 (2022).
55. Chen, S. & Yuan, X. Quantifying the uncertainty of internal variability in future projections of seasonal soil moisture droughts over China. *Sci. Total Environ.* **824**, 153817 (2022).
56. Maher, N., Matei, D., Milinski, S. & Marotzke, J. ENSO change in climate projections: forced response or internal variability?. *Geophys. Res. Lett.* **45**, 398 (2018). 11, 311–390.
57. Rattalino Edreira, J. I. et al. Spatial frameworks for robust estimation of yield gaps. *Nat. Food* **2**, 773–779 (2021).
58. van Bussel, L. G. J. et al. From field to atlas: Upscaling of location-specific yield gap estimates. *Field Crop. Res.* **177**, 98–108 (2015).
59. Yuan, S. et al. Southeast Asia must narrow down the yield gap to continue to be a major rice bowl. *Nat. Food* **3**, 217–226 (2022).
60. Sun, S., Yang, X., Lin, X., Sassenrath, G. F. & Li, K. Winter wheat yield gaps and patterns in China. *Agron. J.* **110**, 319–330 (2018).
61. Liu, B., Wu, L., Chen, X. & Meng, Q. Quantifying the potential yield and yield gap of Chinese wheat production. *Agron. J.* **108**, 1890–1896 (2016).
62. Wu, D., Yu, Q., Lu, C. & Hengsdijk, H. Quantifying production potentials of winter wheat in the North China Plain. *Eur. J. Agron.* **24**, 226–235 (2006).
63. Bai, H. & Tao, F. Sustainable intensification options to improve yield potential and eco-efficiency for rice-wheat rotation system in China. *Field Crop. Res.* **211**, 89–105 (2017).
64. Gou, F. et al. On yield gaps and yield gains in intercropping: Opportunities for increasing grain production in northwest China. *Agr. Syst.* **151**, 96–105 (2017).

65. Zhang, L., Feng, H. & Cao, H. Winter wheat yield gaps across the Loess plateau of China. *Int. J. Plant Prod.* **16**, 1–15 (2022).
66. Gao, Y. et al. Spatial and temporal variations of maize and wheat yield gaps and their relationships with climate in China. *Agr. Water Manag.* **270**, 107714 (2022).
67. Lu, C. & Fan, L. Winter wheat yield potentials and yield gaps in the North China Plain. *Field Crop. Res.* **143**, 98–105 (2013).
68. Chen, Y., Zhang, Z., Tao, F., Wang, P. & Wei, X. Spatio-temporal patterns of winter wheat yield potential and yield gap during the past three decades in North China. *Field Crop. Res.* **206**, 11–20 (2017).
69. Cui, Z. et al. Pursuing sustainable productivity with millions of smallholder farmers. *Nature* **555**, 363–366 (2018).
70. IPCC. *Climate Change 2022: Impacts, Adaptation and Vulnerability. Contribution of Working Group II to the Sixth Assessment Report of the Intergovernmental Panel on Climate Change.* (Cambridge University Press, Cambridge, UK and New York, USA, 2022).
71. Jägermeyr, J. et al. Climate impacts on global agriculture emerge earlier in new generation of climate and crop models. *Nat. Food* **2**, 873–885 (2021).
72. Yang, X. et al. Potential benefits of climate change for crop productivity in China. *Agr. Meteorol.* **208**, 76–84 (2015).
73. Xiao, D. et al. Climate change impact on yields and water use of wheat and maize in the North China Plain under future climate change scenarios. *Agr. Water Manag.* **238**, 106238 (2020).
74. Wang, X. et al. Global irrigation contribution to wheat and maize yield. *Nat. Commun.* **12**, 1235 (2021).
75. Lawes, R. et al. Applying more nitrogen is not always sufficient to address dryland wheat yield gaps in Australia. *Field Crop. Res.* **262**, 108033 (2021).
76. GOBBETT, D. L. et al. Yield gap analysis of rainfed wheat demonstrates local to global relevance. *J. Agric. Sci.* **155**, 282–299 (2017).
77. Hochman, Z., Gobbett, D., Horan, H. & Navarro Garcia, J. Data rich yield gap analysis of wheat in Australia. *Field Crop. Res.* **197**, 97–106 (2016).
78. van Wart, J., Kersebaum, K. C., Peng, S., Milner, M. & Cassman, K. G. Estimating crop yield potential at regional to national scales. *Field Crop. Res.* **143**, 34–43 (2013).
79. van Ittersum, M. K. et al. Can sub-Saharan Africa feed itself?. *Proc. Natl. Acad. Sci.* **113**, 14964–14969 (2016).
80. Rattalino Edreira, J. I. et al. Water productivity of rainfed maize and wheat: A local to global perspective. *Agr. Meteorol.* **259**, 364–373 (2018).
81. Tittonell, P. & Giller, K. E. When yield gaps are poverty traps: The paradigm of ecological intensification in African smallholder agriculture. *Field Crop. Res.* **143**, 76–90 (2013).
82. Tittonell, P., Shepherd, K. D., Vanlauwe, B. & Giller, K. E. Unravelling the effects of soil and crop management on maize productivity in smallholder agricultural systems of western Kenya—An application of classification and regression tree analysis. *Agric. Ecosyst. Environ.* **123**, 137–150 (2008).
83. Zhang, Q., Xu, C., Chen, X. & Zhang, Z. Statistical behaviours of precipitation regimes in China and their links with atmospheric circulation 1960–2005. *Int. J. Climatol.* **31**, 1665–1678 (2011).
84. Zhang, Q., Li, J., Singh, V. P. & Bai, Y. SPI-based evaluation of drought events in Xinjiang, China. *Nat. Hazards* **64**, 481–492 (2012).
85. Chen, J., Huang, Y. & Tang, Y. Quantifying economically and ecologically optimum nitrogen rates for rice production in south-eastern China. *Agric. Ecosyst. Environ.* **142**, 195–204 (2011).
86. Wang, D. J., Liu, Q., Lin, J. H. & Sun, R. J. Optimum nitrogen use and reduced nitrogen loss for production of rice and wheat in the Yangtze Delta Region. *Environ. Geochem. Health.* **26**, 221–227 (2004).
87. Wang, B. et al. Sources of uncertainty for wheat yield projections under future climate are site-specific. *Nat. Food* **1**, 720–728 (2020).
88. Challinor, A. J. et al. A meta-analysis of crop yield under climate change and adaptation. *Nat. Clim. Change* **4**, 287–291 (2014).
89. National Bureau of Statistics. National Bureau of Statistics. <http://www.stats.gov.cn> (accessed 1 April 2023), (2023).
90. Cui, Z. et al. Closing the N-use efficiency gap to achieve food and environmental security. *Environ. Sci. Technol.* **48**, 5780–5787 (2014).
91. Wang, J. et al. Reactive N emissions from cropland and their mitigation in the North China Plain. *Environ. Res.* **214**, 114015 (2022).
92. Zhang, J. J. et al. Nutrient expert improves nitrogen efficiency and environmental benefits for winter wheat in China. *Agron. J.* **110**, 696–706 (2018).
93. Li, H. et al. Effects of different nitrogen fertilizers on the yield, water- and nitrogen-use efficiencies of drip-fertigated wheat and maize in the North China Plain. *Agr. Water Manag.* **243**, 106474 (2021).
94. Zhang, D. et al. The status and distribution characteristics of residual mulching film in Xinjiang, China. *J. Integr. Agr.* **15**, 2639–2646 (2016).
95. Zhang, F. et al. Effect of planting density on canopy structure, microenvironment, and yields of uniformly sown winter wheat. *Agronomy.* **13**, (2023).
96. Wang, K., Su, L. & Wang, Q. Cotton growth model under drip irrigation with film mulching: A case study of Xinjiang, China. *Agron. J.* **113**, 2417–2436 (2021).
97. Lu, J., Carbone, G. J. & Grego, J. M. Uncertainty and hotspots in 21st century projections of agricultural drought from CMIP5 models. *Sci. Rep.* **9**, 4922 (2019).
98. Jin, X. et al. A review of data assimilation of remote sensing and crop models. *Eur. J. Agron.* **92**, 141–152 (2018).
99. de Bie C. A. J. M. Comparative performance analysis of agro-ecosystems. Ph D thesis, Wageningen University, Wageningen, Netherlands, 2000.
100. Shen, J. et al. Transforming agriculture in China: From solely high yield to both high yield and high resource use efficiency. *Glob. Food Secur.* **2**, 1–8 (2013).
101. Bai, H., Wang, J., Fang, Q. & Huang, B. Does a trade-off between yield and efficiency reduce water and nitrogen inputs of winter wheat in the North China Plain?. *Agr. Water Manag.* **233**, 106095 (2020).
102. Wang, C., Li, X., Gong, T. & Zhang, H. Life cycle assessment of wheat-maize rotation system emphasizing high crop yield and high resource use efficiency in Quzhou County. *J. Clean. Prod.* **68**, 56–63 (2014).
103. van Wart, J. et al. Use of agro-climatic zones to upscale simulated crop yield potential. *Field Crop. Res.* **143**, 44–55 (2013).
104. Liu, B., Chen, X., Meng, Q., Yang, H. & van Wart, J. Estimating maize yield potential and yield gap with agro-climatic zones in China—Distinguish irrigated and rainfed conditions. *Agr. Meteorol.* **239**, 108–117 (2017).
105. Yu, Q. et al. A cultivated planet in 2010 – Part 2: The global gridded agricultural-production maps. *Earth Syst. Sci. Data* **12**, 3545–3572 (2020).
106. Chen, S. et al. Using support vector machine to deal with the missing of solar radiation data in daily reference evapotranspiration estimation in China. *Agr. Meteorol.* **316**, 108864 (2022).
107. Dai, Y. et al. Development of a China Dataset of soil hydraulic parameters using pedotransfer functions for land surface modeling. *J. Hydrometeorol.* **14**, 869–887 (2013).
108. Wieder, W. R., Boehnert, J. & Bonan, G. B. Evaluating soil biogeochemistry parameterizations in Earth system models with observations. *Glob. Biogeochem. Cy.* **28**, 211–222 (2014).
109. Jones, J. W. et al. The DSSAT cropping system model. *Eur. J. Agron.* **18**, 235–265 (2003).
110. Ghasemi-Saadatabadi, F. et al. Improving prediction accuracy of CSM-CERES-Wheat model for water and nitrogen response using a modified Penman-Monteith equation in a semi-arid region. *Field Crop. Res.* **312**, 109381 (2024).

111. Lv, Z., Liu, X., Cao, W. & Zhu, Y. A Model-Based Estimate of Regional Wheat Yield Gaps and Water Use Efficiency in Main Winter Wheat Production Regions of China. *Sci. Rep.* **7**, 6081 (2017).
112. Liu, J. et al. Modeling wheat nutritional quality with a modified CERES-wheat model. *Eur. J. Agron.* **109**, 125901 (2019).
113. Chen, S. et al. Comparisons among four different upscaling strategies for cultivar genetic parameters in rainfed spring wheat phenology simulations with the DSSAT-CERES-Wheat model. *Agr. Water Manag.* **258**, 107181 (2021).
114. Kendall, M. G. Rank Correlation Methods; 1949.
115. Mann, H. B. Nonparametric tests against trend. *Econometrica* **13**, 245 (1945).
116. Gidden, M. J. et al. Global emissions pathways under different socioeconomic scenarios for use in CMIP6: a dataset of harmonized emissions trajectories through the end of the century. *Geosci. Model Dev.* **12**, 1443–1475 (2019).
117. Liu, D. L. & Zuo, H. Statistical downscaling of daily climate variables for climate change impact assessment over New South Wales, Australia. *Clim. Change* **115**, 629–666 (2012).
118. Gong, K. et al. Influences of climate change on carbon and water fluxes of the ecosystem in the Qinling Mountains of China. *Ecol. Indic.* **166**, 112504 (2024).
119. Ladha, J. K., Pathak, H., J. Krupnik, T., Six, J. & van Kessel, C. Efficiency of fertilizer nitrogen in cereal production: retrospects and prospects. *Advances in Agronomy*: Academic Press; 2005. 85–156.
120. Hartmann, T. E. et al. Yield and N use efficiency of a maize–wheat cropping system as affected by different fertilizer management strategies in a farmer’s field of the North China Plain. *Field Crop. Res.* **174**, 30–39 (2015).
121. Terry Howell, B. A. S. *Encyclopedia of Water Science*. (New York: Marcel Dekker Inc, 2003).
122. Qin, W., Hu, C. & Oenema, O. Soil mulching significantly enhances yields and water and nitrogen use efficiencies of maize and wheat: a meta-analysis. *Sci. Rep.* **5**, 16210 (2015).
123. Hawkins, E. & Sutton, R. The potential to narrow uncertainty in regional climate predictions. *B. Am. Meteorol. Soc.* **90**, 1095–1108 (2009).
124. Wootten, A., Terando, A., Reich, B. J., Boyles, R. P. & Semazzi, F. Characterizing sources of uncertainty from global climate models and downscaling techniques. *J. Appl. Meteorol. Clim.* **56**, 3245–3262 (2017).
125. Zhou, T., Lu, J., Zhang, W. & Chen, Z. The sources of uncertainty in the projection of global land monsoon precipitation. *Geophys. Res. Lett.* **47**, e2020G–e88415G (2020).

Acknowledgements

This research was partially supported by the National Natural Science Foundation of China (No. 52079115), the National Key Research and Development Program of China (No. 2021YFD1900700), the “111 Project” (No. B12007) of China and the National Key Research and Development Program of China (2016YFD0300100).

Author contributions

K.Y.G. contributed to writing the original manuscript. L.B.R., Y.H.Z. and X.W. performed the experiments. F.Y.D. and X.L. participated in data analysis. Z.H.H., T.C.J. and S.C. contributed discussion. H.F., Q.Y. supervised the project. Funding for the project was provided by W.B.Z. and J.Q.H. All authors contributed to the reviewing, editing, and improvement of the manuscript.

Competing interests

The authors declare no competing interests.

Additional information

Supplementary information The online version contains supplementary material available at <https://doi.org/10.1038/s43247-025-02280-7>.

Correspondence and requests for materials should be addressed to Wenbin Zhou or Jianqiang He.

Peer review information *Communications Earth & Environment* thanks Yadunath Bajgai and the other, anonymous, reviewer(s) for their contribution to the peer review of this work. Primary Handling Editors: Ariel Soto-Caro and Mengjie Wang. A peer review file is available.

Reprints and permissions information is available at <http://www.nature.com/reprints>

Publisher’s note Springer Nature remains neutral with regard to jurisdictional claims in published maps and institutional affiliations.

Open Access This article is licensed under a Creative Commons Attribution-NonCommercial-NoDerivatives 4.0 International License, which permits any non-commercial use, sharing, distribution and reproduction in any medium or format, as long as you give appropriate credit to the original author(s) and the source, provide a link to the Creative Commons licence, and indicate if you modified the licensed material. You do not have permission under this licence to share adapted material derived from this article or parts of it. The images or other third party material in this article are included in the article’s Creative Commons licence, unless indicated otherwise in a credit line to the material. If material is not included in the article’s Creative Commons licence and your intended use is not permitted by statutory regulation or exceeds the permitted use, you will need to obtain permission directly from the copyright holder. To view a copy of this licence, visit <http://creativecommons.org/licenses/by-nc-nd/4.0/>.

© The Author(s) 2025